Developmental Biology 453 (2019) 86–104

Contents lists available at ScienceDirect

Developmental Biology

journal homepage: www.elsevier.com/locate/developmentalbiology

Lens differentiation is characterized by stage-specific changes in chromatin accessibility correlating with differentiation state-specific gene expression☆

Joshua Disatham [a], Daniel Chauss [b], Rifah Gheyas [c], Lisa Brennan [a], David Blanco [a], Lauren Daley [a], A. Sue Menko [c], Marc Kantorow [a,*]

[a] Department of Biomedical Science, Charles E. Schmidt College of Medicine, Florida Atlantic University, Boca Raton, FL, USA
[b] National Institute of Diabetes and Digestive and Kidney Diseases, National Institutes of Health, Bethesda, MD, USA
[c] Department of Pathology, Anatomy and Cell Biology, Thomas Jefferson University, Philadelphia, PA, USA

A B S T R A C T

Changes in chromatin accessibility regulate the expression of multiple genes by controlling transcription factor access to key gene regulatory sequences. Here, we sought to establish a potential function for altered chromatin accessibility in control of key gene expression events during lens cell differentiation by establishing genome-wide chromatin accessibility maps specific for four distinct stages of lens cell differentiation and correlating specific changes in chromatin accessibility with genome-wide changes in gene expression. ATAC sequencing was employed to generate chromatin accessibility profiles that were correlated with the expression profiles of over 10,000 lens genes obtained by high-throughput RNA sequencing at the same stages of lens cell differentiation. Approximately 90,000 regions of the lens genome exhibited distinct changes in chromatin accessibility at one or more stages of lens differentiation. Over 1000 genes exhibited high Pearson correlation coefficients ($r > 0.7$) between altered expression levels at specific stages of lens cell differentiation and changes in chromatin accessibility in potential promoter (−7.5kbp/+2.5kbp of the transcriptional start site) and/or other potential cis-regulatory regions (±10 kb of the gene body). Analysis of these regions identified consensus binding sequences for multiple transcription factors including members of the TEAD, FOX, and NFAT families of transcription factors as well as HIF1a, RBPJ and IRF1. Functional mapping of genes with high correlations between altered chromatin accessibility and differentiation state-specific gene expression changes identified multiple families of proteins whose expression could be regulated through changes in chromatin accessibility including those governing lens structure (BFSP1,BFSP2), gene expression (Pax-6, Sox 2), translation (TDRD7), cell-cell communication (GJA1), autophagy (FYCO1), signal transduction (SMAD3, EPHA2), and lens transparency (CRYBB1, CRYBA4). These data provide a novel relationship between altered chromatin accessibility and lens differentiation and they identify a wide-variety of lens genes and functions that could be regulated through altered chromatin accessibility. The data also point to a large number of potential DNA regulatory sequences and transcription factors whose functional analysis is likely to provide insight into novel regulatory mechanisms governing the lens differentiation program.

1. Introduction

A requirement for the successful completion of the cellular differentiation events leading to formation of specialized tissues and organs is the expression of critical genes at distinct stages of their cellular differentiation programs. Among the many mechanisms regulating the expression of specific genes during cellular differentiation, transcriptional control through binding of transcription factors to key cis-regulatory sequences is a major control pathway (Chandler and Jones, 1988; Harrison, 1990; Roy and Kundu, 2014). The function of transcription factors can be controlled through access to cis-regulatory sequences as a consequence of chromatin accessibility changes resulting from altered nucleosome occupancy at specific DNA sequences (Jiang and Pugh, 2009). Although it is well-established that changes in chromatin accessibility regulate a wide-variety of genes (Lawrence et al., 2016; Rudnizky et al., 2017; Venkatesh and Workman, 2015), the potential role for altered chromatin accessibility in the regulation of those gene expression events required for the formation of organs and specialized tissues remains to be fully elucidated.

Studies on the role of altered chromatin accessibility in the differentiation of organs and specialized tissues have been limited by a scarcity of robust model systems. A well-established model system is the lens, whose function is to focus light onto the retina where visual information is transmitted to the brain (Cvekl and Ashery-Padan, 2014; Cvekl and Zhang, 2017; Piatigorsky, 1981). A major feature of the lens is that, unlike many tissues, it grows both embryologically and throughout adult life through execution of a continuous cellular differentiation program reflected in morphologically distinct populations of cells at distinct stages

☆ Supported by NIH, NEI grant EY026478 (MK and ASM).
* Corresponding author. Charles E. Schmidt College of Medicine, Florida Atlantic University, Boca Raton, FL, 33467, USA.
E-mail address: mkantoro@health.fau.edu (M. Kantorow).

https://doi.org/10.1016/j.ydbio.2019.04.020
Received 6 March 2019; Received in revised form 16 April 2019; Accepted 16 April 2019
Available online 25 May 2019

of the lens differentiation program (Menko, 2002). These cell populations include a monolayer of undifferentiated epithelial cells at the center of the lens anterior (EC cells), a monolayer of replicative epithelial cells at the lens equator that withdraw from the cell cycle to initiate differentiation (EQ cells), a zone of newly formed fiber cells at the lens cortex that undergo a series of remodeling events including elongation (FP cells) and finally, a core of elongated fiber cells from which all organelles are eliminated and which make up the bulk of the lens (FC cells) (Bassnett et al., 2011; Menko, 2002; Piatigorsky, 1981; Audette et al., 2017; Chauss et al., 2014a; Cheng et al., 2017; Costello et al., 2013; FitzGerald, 2009; Mathias et al., 2010; Perng et al., 2007; Rao and Maddala, 2006; Robinson, 2006; Lovicu and McAvoy, 2005; Brennan et al., 2018). These differentiation state-specific and morphologically distinct populations of lens cells can be isolated in quantities sufficient for molecular and biochemical analysis by microdissection (Chauss et al., 2014; Walker and Menko, 1999).

Lens cell differentiation is hallmarked by the expression of critical regulatory and structural genes at key stages of the lens cell differentiation program (Cvekl and Zhang, 2017) (Yang et al., 2010)). Consistently, recent studies have employed high-throughput mRNA-sequencing to identify the range and spectrum of genes expressed at distinct stages of lens differentiation (Chauss et al., 2014; Zhao et al., 2018a). The differentiation state-specific expression patterns of these genes suggests that specific regulatory mechanisms operate to govern their expression levels at specific stages of the lens cell differentiation program. Consistently, previous studies have identified multiple transcription factors (Cvekl and Zhang, 2017), growth factors (Lovicu and McAvoy, 2005; Robinson, 2006), translational regulatory proteins (Lachke et al., 2011), and signal transduction pathways (McAvoy et al., 2017; Menko, 2002) that are required for their differentiation state-specific expression patterns.

An unexplored mechanism that could play a critical role in regulating the differentiation state-specific expression of critical genes during lens cell differentiation is alterations in chromatin accessibility that could control the binding and activity of important transcription factors at

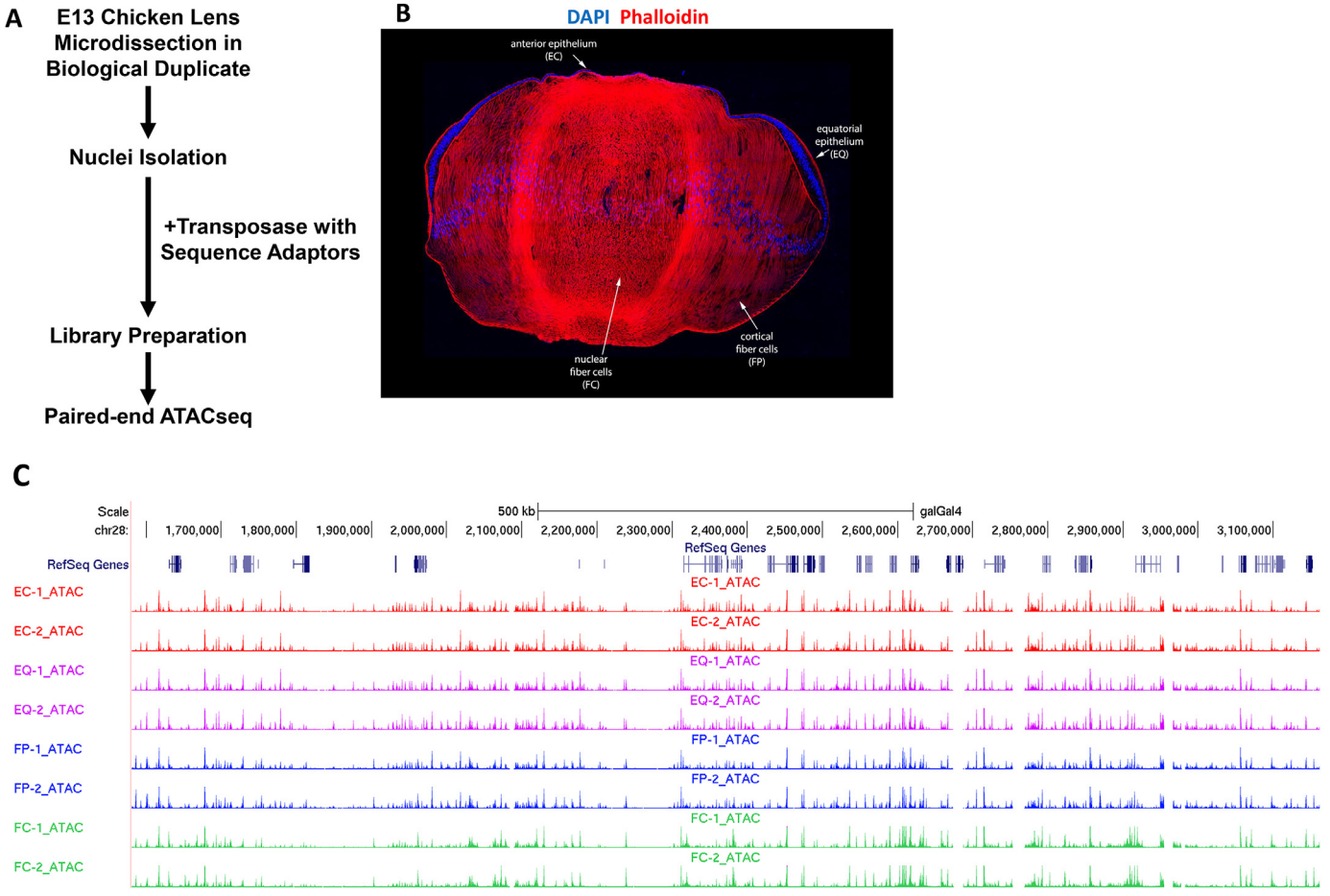

Fig. 1. Chromatin accessible DNA regions cluster in potential cis-regulatory regions of the chick eye lens genome. A. Experimental Design: Duplicate pools (n = 100) of E13 Embryonic chick lenses were micro-dissected into regions corresponding with progressive stages of lens cell differentiation including central epithelium (EC), equatorial epithelium (EQ), newly formed fiber cells (FP), and mature fiber cells (FC). Samples were analyzed by ATAC sequencing as described in methods. A total of 89,904 chromatin accessible regions were identified (Supplementary Table 1) B. Day 13 embryonic chick lenses stained with phalloidin and DAPI with labeled microdissected regions. C. Representative ATAC sequencing tracks derived for chromosome 28 (1,580,876–3,161,751) showing multiple accessible chromatin peaks throughout the indicated chromosomal region. Gene bodies are shown in the top most track labeled Refseq Genes (dark blue). Red peaks represent chromatin accessible regions identified in undifferentiated quiescent central lens epithelial cells (EC). Purple peaks represent chromatin accessible regions identified in differentiating lens epithelial cells that first proliferate and subsequently exit the cell cycle (EQ). Light blue peaks represent chromatin accessible regions identified in actively differentiating nascent lens fiber cells (FP). Green peaks represent chromatin accessible regions identified in terminally differentiated core lens fiber cells (FC). D. Distribution of sites of chromatin accessibility within 5kbp of Transcription Start Sites (TSS) and within 2 kbp of Genebodies for each differentiation-stage replicate. E. Locations of chromatin accessibility sites (ATAC-seq peaks) relative to Promoters (−7.5kbp to +2.5kbp of the TSS), Genebodies (contained within the gene sequence) and Intergenic regions of 10,698 annotated genes established for each stage of lens cell differentiation (EC, EQ, FP and FC). “Control” represents the computer-generated random distribution of peaks against the same annotations. Relative percentage differences between chromatin accessible sites in Promoters, Genebodies, and Intergenic Regions of each differentiation-stage specific lens region relative to the same three regions in the randomly generated “Control”.

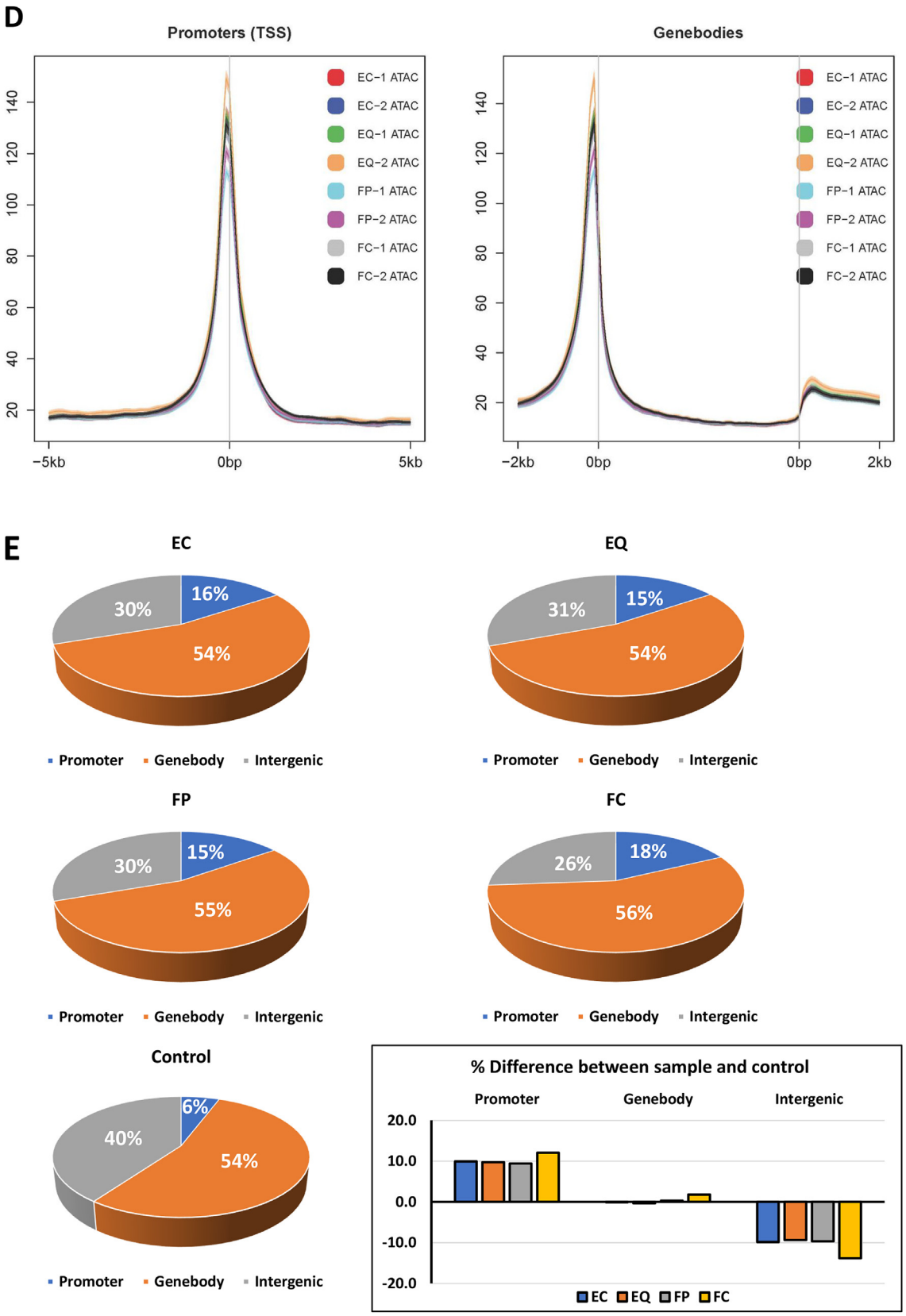

Fig. 1. (*continued*).

specific stages of the lens differentiation program. In support of this possibility, the transcript levels of the lens-specific gene αA-crystallin have been previously linked with alterations in chromatin accessibility (Kantorow et al., 1993).

To investigate the potential relationship between altered chromatin accessibility and the differentiation state-specific expression of critical lens genes, we employed ATAC sequencing to establish genome-wide chromatin accessibility maps specific for distinct stages of lens differentiation and we correlated the identified changes in chromatin accessibility with the differentiation state-specific expression profiles of over 10,000 genes. The resulting data establish a novel relationship between altered chromatin accessibility and lens cell differentiation, they identify a wide-variety of lens genes and functions that could be regulated during lens cell differentiation through changes in chromatin accessibility and they implicate a differentiation-specific function for a large number of previously unidentified DNA regulatory sequences and transcription factors.

2. Methods

2.1. Lens microdissection

Lenses were isolated from chicken embryos (B&E Eggs, York Springs, PA; Poultry Futures) at embryonic day 13 and 100 lenses microdissected into four differentiation-stage specific regions of the lens (Fig. 1A) including central anterior epithelial cells (EC), equatorial epithelial cells (EQ), cortical fiber cells (FP), and central fiber cells (FC) as previously described (Chauss et al., 2014; Walker and Menko, 1999). The resulting microdissected tissues were pooled and frozen in CryoStor CS10 cryspreservation media containing 10% DMSO (Stemcell, Vancouver, Canada) and stored at −80C as previously described (Corces et al., 2017).

2.2. ATAC sequencing

ATAC sequencing (Transposase-Accessible Chromatin with high throughput sequencing) was performed on two independently prepared samples of each stage of lens differentiation as described (Buenrostro et al., 2013). Briefly, each of the frozen pooled samples were thawed in a 37 °C water bath, pelleted, washed with cold PBS, and tagmented (Buenrostro et al., 2013), with some modifications (Corces et al., 2017). Cell pellets were resuspended in lysis buffer, pelleted, and tagmented using the enzyme and buffer provided in the Nextera Library Prep Kit (Illumina). Tagmented DNA was then purified using the MinElute PCR purification kit (Qiagen), amplified with 10 cycles of PCR, and purified. The resulting material was quantified using the KAPA Library Quantification Kit for Illumina platforms (KAPA Biosystems), and sequenced with PE42 sequencing on the NextSeq 500 sequencer (Illumina). Reads were aligned to the chicken genome (galGal4) using the BWA algorithm (mem mode; default settings). Our ATAC sequencing was normalized for total nuclear DNA isolated from each of the four differentiation states analyzed. Duplicate reads were removed and only reads mapping as matched pairs and uniquely mapped reads (mapping quality ≥ 1) were used for further analysis. The 8 samples were normalized to the same number of unique alignments (by downsampling to 38.4 million reads). Alignments were extended in silico at their 3′-ends to a length of 200 bp and assigned to 32-nt bins along the genome. The resulting histograms (genomic "signal maps") were stored in bigWig files. Peaks were identified using the MACS 2.1.0 algorithm at a cutoff of p-value 1e-7, without control file, and with the -nomodel option. Signal maps and peak locations were used as input data to Active Motifs proprietary analysis program which creates Excel tables containing detailed information on sample comparison, peak metrics, peak locations and gene annotations. To compare peak metrics between 2 or more samples, overlapping intervals were grouped into "Merged Regions", which are defined by the start coordinate of the most upstream Interval and the end coordinate of the most downstream Interval. Merged regions found in only one sample of a biological duplicate were excluded from the rest of the analysis. Peaks were annotated to the galGal4 genome and visualized in UCSC Genome Browser (http://genome.ucsc.edu/s/jdisatha/galGal4atacsave).

2.3. Integration of ATAC seq and mRNA seq data

ATAC-seq data was compared with mRNA-seq data obtained from two independently isolated sets of the same microdissected differentiation-stage specific regions described above from 100 E13 chick lenses prepared as above (Chauss et al., 2014). Total RNA was analyzed for quality and subjected to Illumina mRNA directional sequencing library preparation (Illumina, San Diego, CA). Total RNA was also analyzed for quality upon completion of library preparation using the Agilent Technologies 2100 Expert Bioanalyzer (Santa Clara, CA). Sequencing and analysis are further described in (Chauss et al., 2014). Gene annotations matched to both ATAC-seq and RNA-seq datasets were further analyzed.

2.4. Transcription factor sequence analysis in MEME-suite

Transcription factor binding motif analysis was performed in Motif-based sequence analysis tools (MEME-suite 5.0.3) (Bailey et al., 2009) using the AME tool (Analysis of Motif Enrichment) (McLeay and Bailey, 2010).

2.5. Computational analysis

Quantification of chromatin accessibility was established for each gene annotation at each stage of lens differentiation. The average peak intensity was calculated for all peak regions within −7.5kbp/+2.5kbp of the transcription start site (value labeled as "promoter") and within ± 10kbp of the gene body (value labeled as "proximal to genebody"). The average calculated regional intensity values were compared to establish changes in chromatin accessibility for each gene at each stage of lens differentiation. Chromatin accessibility values (calculated as above) and gene expression levels (as FPKM calculated values) for each gene at each stage of lens differentiation were correlated using Pearson's correlation coefficient analysis. Chi-square and Pearson correlation coefficient statistical analyses were performed in R. A cutoff threshold of >0.7 was defined as "high" correlation. All heatmaps shown were generated with the Morpheus tool (https://software.broadinstitute.org/morpheus). Batch gene analysis was executed via the pantherdb gene list analysis tool set to Gallus gallus (Mi et al., 2017) to determine statistically over-represented biological processes. The "GO biological process complete" was used as the "Annotation Data Set". Test type was set to Fisher's Exact. Correction was set to "Calculate False Discovery Rate". Only biological processes with FDR adjusted p-value < 0.05 were reported. Biological processes associated with non-lens tissues were not included in the results. The AME tool from MEME-Suite (McLeay and Bailey, 2010) was used to determine statistically overrepresented transcription factor binding motifs. DNA sequences corresponding to open chromatin regions were extracted from UCSC Genome Browser Table Browser tool (Karolchik et al., 2004) and used as input for the AME tool. Shuffled input sequences were used as control sequences to distinguish significant transcription factor motifs from statistical noise. The shuffled input sequences are a computer-generated background from which the sequences of interest can be measured against to find statistically significant over-represented transcription factor motifs. JASPAR (non-redundant) CORE Vertebrates transcription factor motif database (Khan et al., 2018) was used as the motifs input for the AME tool. All other settings were set to the default AME tool settings. Motifs with an E-value > 0.05 were excluded from further analysis. The MAST tool from MEME-Suite (Bailey and Gribskov, 1998) was used to identify the most statistically significant potential transcription factor binding sites within regions of altered chromatin accessibility matched to five selected genes. DNA sequences corresponding to open chromatin regions matched to the selected genes were extracted from UCSC Genome Browser Table Browser tool and used as input for the MAST tool. 25 Transcription factor motifs from the

JASPAR (non-redundant) CORE Vertebrates database and detected by the AME tool (E-value < 0.05) was used as the motifs input for the MAST tool. All other settings were set to the default MAST tool settings. Potential transcription factor sites with a p-value < 1E-4 were excluded from further analysis. Some transcription factors had multiple potential binding sites with p-value < 1E-4 matched to one gene. In these situations, only the most statistically significant (lowest p-value) binding site was reported.

3. Results

3.1. Differences in chromatin accessibility characterize distinct stages of the lens cell differentiation program

To map the chromatin accessibility profile of the lens genome at distinct stages of lens cell differentiation embryonic day 13 (E13) lenses (100 per sample) were microdissected into four differentiation stage-specific regions (EC, EQ, FP, FC) and duplicate samples of each region were subjected to ATAC sequencing as shown in Fig. 1A. Regions of the lens analyzed included morphological zones containing a monolayer of undifferentiated epithelial cells of the anterior central region of the lens facing the light path (EC), epithelial cells of the lens equator undergoing proliferation followed by cell cycle exit to initiate differentiation (EQ), nascent fiber cells of the lens cortex undergoing cellular elongation (FP) and terminally differentiated fiber cells that become organelle-free in the lens core (FC) (Fig. 1B). ATAC sequencing analysis of duplicate samples of each region identified 89,904 transposase TN5-accessible DNA sequences in the chick lens genome (Supplementary Table 1). Genomic alignment of the identified chromatin accessible regions was employed to assemble chromatin accessibility profiles specific for each stage of lens cell differentiation (can be viewed at http://genome.ucsc.edu/s/jdisatha/galGal4atacsave). An example is shown in Fig. 1C that depicts

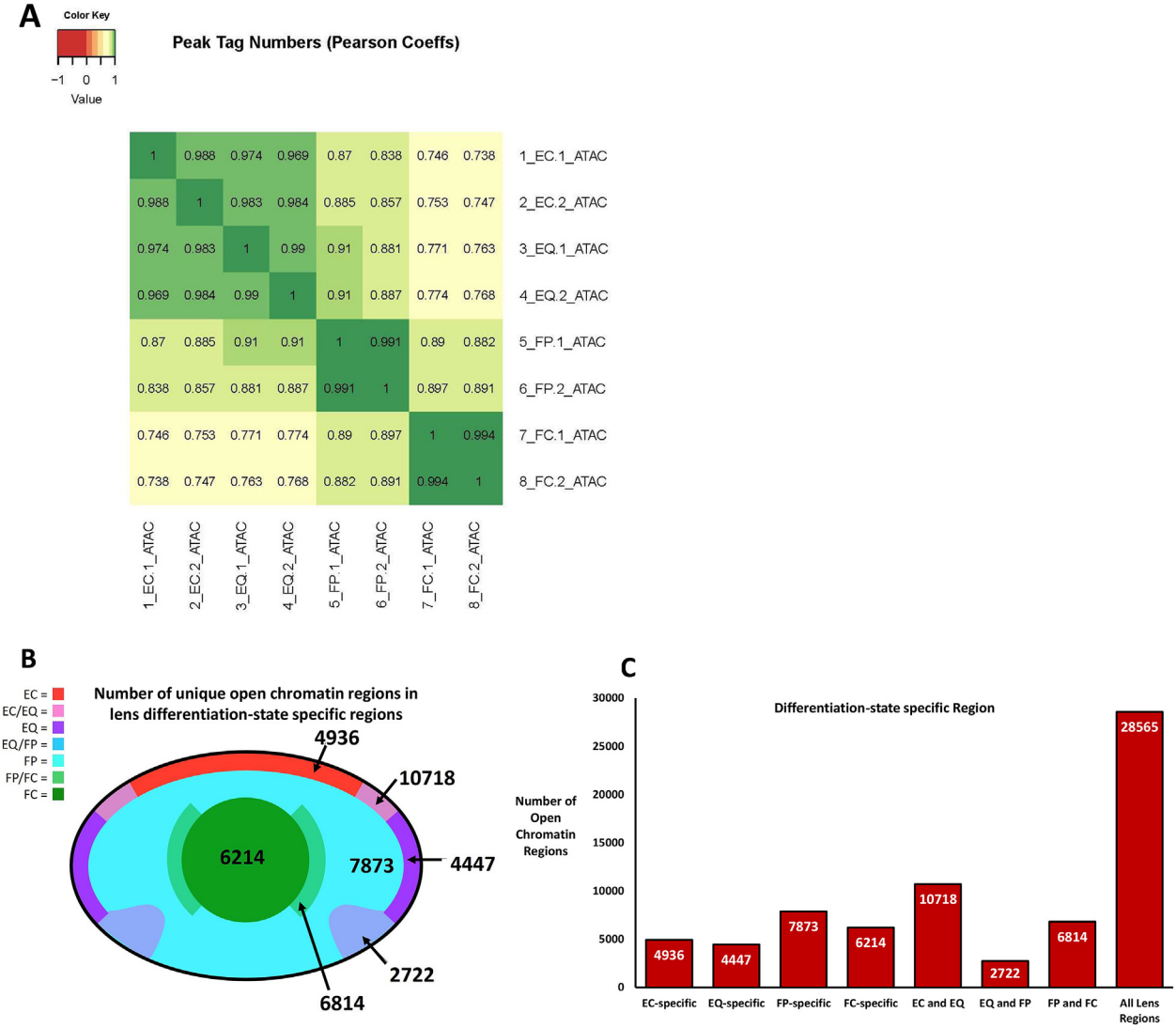

Fig. 2. Specific stages of lens cell differentiation are marked by key differences in chromatin accessibility most abundant between differentiating lens epithelial cells and nascent lens fiber cells. A. Distribution of peak tag numbers between biological duplicates of samples (intra-sample variation), and between lens micro-dissected regions (inter-sample variation) indicating low intrasample variation and significant intersample differences that increase as lens cell differentiation proceeds (EC to EQ, EQ to FP, FP to FC). B. Number of differentiation stage-specific sites of chromatin accessibility (ATACseq peaks) detected in each micro-dissected lens region. Peaks that were found in two adjacent lens regions are also indicated. C. Bar graph of the number of altered sites of chromatin accessibility determined for each stage of lens cell differentiation. Number of sites common to adjacent stages of lens differentiation and common to all four stages of lens differentiation are also included. D. Differential analysis of sites of chromatin accessibility reveals altered levels of chromatin accessibility (open or closed) in specific stages of lens cell differentiation analyzed by pairwise comparison and displayed as volcano plots (red dots indicate sites with |Log2 fold change average peak intensity| > 1, FDR adj p-value < 0.05). A differential analysis of sites of chromatin accessibility differences common to combined epithelial cell stages of differentiation and combined fiber cell states of differentiation is also shown for comparison (E vs. F).

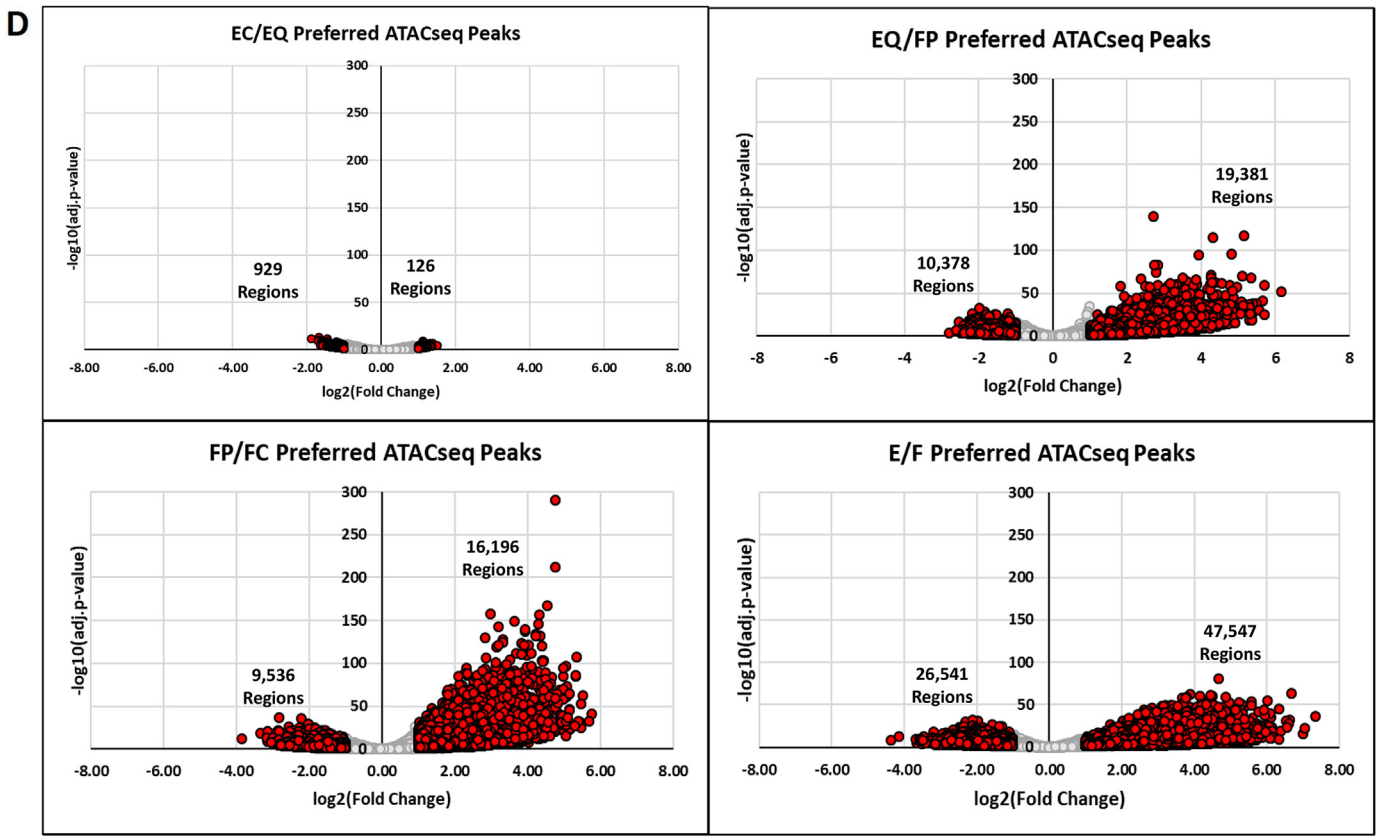

Fig. 2. (*continued*).

representative ATAC seq tracks detected at chromosome 28 between 1,580,876bp and 3,161,751bp at each stage of lens cell differentiation. The vast majority of chromatin accessible regions were contained within 5 kb of transcription start sites (TSS) or within 2 kb of their gene bodies of 10,698 annotated Gallus gallus genes (Fig. 1D). 15–18% of DNA accessible regions were found within ± 5 kb of the transcription start site of each gene as calculated for each stage of lens differentiation (Fig. 1E). The data was normalized for genomic size and compared to a simulated control sample with randomly distributed ATAC-peaks. This analysis revealed an asymmetric positive distribution of chromatin accessible sites near transcriptional start-sites and a negative distribution of chromatin accessible sites in intergenic regions (Fig. 1E). These data suggest a higher density of chromatin accessible regions in potential DNA regulatory sequences upstream of transcriptional start sites relative to intergenic DNA regions.

In order to investigate the chromatin accessibility differences between differentiation stage-specific regions, we performed pairwise comparison of peak tag numbers between individual stages of lens differentiation and the data was analyzed by Pearson's correlation analysis. The analysis revealed a very high ($r > 0.98$) Pearson correlation coefficient between biological duplicate samples indicating low intrasample variation (Fig. 2A). Pairwise comparison of peak tag numbers between epithelial cell-specific (EC vs. EQ) or fiber cell-specific regions (FP vs. FC) revealed greater Pearson's correlation coefficients for epithelial cell to epithelial cell and fiber to fiber cell comparisons suggesting that chromatin accessible regions are more similarly conserved between epithelial cells or between fiber cells relative to epithelial cell to fiber cell cross-comparisons (Fig. 2A). Step-wise comparison of individual lens differentiation stage-specific regions indicated a higher similarity between adjacent lens regions (Fig. 2A) relative to non-adjacent regions suggesting that differences in chromatin accessibility characterize the progressive stages of lens differentiation from undifferentiated lens epithelial cells (EC) to terminally differentiated lens fiber cells (FC).

Of the 89,904 open chromatin regions detected for the combined zones of the lens (Supplementary Table 1), 26% of chromatin accessible regions contained a detectable ATAC peak in only a single stage of lens cell differentiation. Specifically, 5.49% of chromatin accessible regions contained a detectable ATAC peak only in undifferentiated central lens epithelial cells (EC), 4.95% of chromatin accessible regions contained a detectable ATAC peak only in lens epithelial cells initiating their differentiation program at the lens equator (EQ), 8.76% of chromatin accessible regions contained a detectable ATAC peak only in newly formed lens fiber cells undergoing remodeling (FP), and 6.91% of chromatin accessible regions contained a detectable ATAC peak only in terminally differentiated lens fiber cells of the lens core (FC) (Fig. 2B and C). The remaining 74% of chromatin accessible regions contained a detectable ATAC peak in at least two of the four stages of lens cell differentiation. Specifically, 11.92% of chromatin accessible regions contained a detectable ATAC peak only in both epithelial cell stages of differentiation (EC and EQ), 7.58% of chromatin accessible regions contained a detectable ATAC peak only in both fiber cell stages of differentiation (FP and FC), and 3.03% of chromatin accessible regions contained a detectable ATAC peak only in both differentiating lens epithelial cells and nascent lens fiber cells (EQ and FP) (Fig. 2B and C). Additionally, a large majority of open chromatin regions (31.77%) contained a detectable ATAC peak in all four stages of lens cell differentiation (Fig. 2C). The observation that a majority of chromatin accessible regions (74%) were detected in at least two of the four differentiation state-specific regions suggests that most differences in chromatin accessibility patterns are not based on a simple binary definition of “open” or “closed” chromatin. Instead, individual chromatin accessible regions detected in multiple differentiation state-specific regions of the lens are relatively more open in one lens region compared to another region of the lens in which the chromatin accessible region is relatively more closed. Thus, in order to fully characterize chromatin accessibility changes during lens cell differentiation, we quantified ATAC peak intensities at all 89,904 individual

chromatin accessible sites by calculating average peak value intensities of these unique sites and analyzed the differences in peak intensity by pairwise comparison of adjacent lens differentiation-specific zones (Supplementary Table 1). Volcano plots of the data were prepared based on mean peak intensities using a |log 2 fold change cutoff| of >1 and FDR adjusted $p < 0.05$ (Fig. 2D). Consistent with the data showing unique chromatin maps for differentiation stage-specific regions of the lens (Fig. 2 B and C), 929 chromatin accessible regions exhibited higher peak intensities in undifferentiated lens epithelial cells (EC) relative to differentiating lens epithelial cells (EQ); 126 chromatin accessible regions exhibited higher peak intensities in differentiating lens epithelial cells (EQ) relative to undifferentiated lens epithelial cells (EC); 10,378 chromatin accessible regions exhibited higher peak intensities in differentiating lens epithelial cells (EQ) relative to nascent lens fiber cells (FP); 19,381 chromatin accessible regions exhibited higher peak intensities in nascent lens fiber cells (FP) relative to differentiating lens epithelial cells (EQ); 9,536 chromatin accessible regions exhibited higher peak intensities in nascent lens fiber cells (FP) relative to terminally differentiated lens fiber cells (FC); 16,196 chromatin accessible regions exhibited higher peak intensities in terminally differentiated lens fiber cells (FC) relative to nascent lens fiber cells (FP). Analysis of mean peak intensity differences between combined lens epithelial cell zones and combined lens fiber cell zones revealed 26,541 chromatin accessible regions that exhibited higher peak intensities in lens epithelial cells (EC and EQ) relative to lens fiber cells (FP and FC) and 47,547 chromatin accessible regions that exhibited higher peak intensities in lens fiber cells (FP and FC) relative to lens epithelial cells (EC and EQ). These data further confirm the differences in chromatin accessibility between different differentiation stage-specific zones of the lens shown in Fig. 2B and C and they provide evidence that the majority of chromatin accessibility differences arise during the transition from differentiating lens epithelial cells (EQ) to nascent lens fiber cells (FP) also called the lens transition zone.

3.2. *Chromatin accessibility changes correlate with the transcript levels of a wide range of lens differentiation markers and other important genes*

In order to examine the specific chromatin accessibility changes characteristic of individual genes, we quantified chromatin accessibility proximal to the transcription start site (−7.5kbp/+2.5kbp of the TSS) for 10,423 annotated genes across the four progressive stages of lens cell differentiation (Supplementary Table 2A). We used Pearsons correlation analysis to compare chromatin accessibility changes proximal to the TSS with gene expression changes obtained from RNAseq data for the same 10,423 annotated genes (Chauss et al., 2014). A representation of this analysis can be seen in Fig. 3. We quantified chromatin accessibility changes proximal to the TSS of the gene encoding the lens structural protein beaded filament protein 1 (BFSP1) (Fig. 3A and B) and found that chromatin accessibility increases as lens cell differentiation proceeds from undifferentiated lens epithelial cells (EC) to terminally differentiated lens fiber cells (FC). In parallel with increasing regions of chromatin accessibility, BFSP1 gene expression levels also increase as lens cell differentiation proceeds (Fig. 3C). Using Pearsons correlation analysis, we found a high correlation ($r = 0.94$) between chromatin accessibility changes and gene expression levels of BFSP1 throughout the four progressive stages of lens differentiation (Fig. 3D). Similar trends were also observed for the lens structural protein beaded filament protein 2 (BFSP2) (Fig. 3E–H), gamma crystallin (CRYGN) (Fig. 3I-L), and delta crystallin (ASL1) (Fig. 3Q–T) that exhibited increased zones of chromatin accessibility in parallel with increased gene expression during lens cell differentiation. By contrast opposite trends were observed for the transcription factor paired box 6 (PAX6) (Fig. 3M–P). A high correlation ($r > 0.7$) between chromatin accessibility changes and gene expression level changes were calculated for all four genes. Analysis of all 10,423 annotated genes, revealed that 31.87% (3322 genes) exhibited a high correlation ($r > 0.7$) between chromatin accessibility changes proximal to transcription start sites and their specific gene expression level changes during lens cell differentiation. These data suggest that changes in chromatin accessibility are linked to the expression of the analyzed genes and implicate chromatin accessibility in the regulation of these genes during lens cell differentiation.

To establish a relationship between alterations in chromatin accessibility during lens differentiation and the expression levels of key lens differentiation markers and other genes, we compared the percentage of genes exhibiting positive correlations between chromatin accessibility changes ($r > 0.7$) and gene expression levels (|Log2 fold change FPKM| > 1 between any two adjacent lens differentiation state-specific regions and false discovery rate adjusted p-value < 0.05) during lens cell differentiation relative to the percentage of genes that exhibited positive correlations between altered chromatin accessibility ($r > 0.7$) but did not exhibit changes in expression levels (Fig. 4A). This analysis revealed that a higher percentage of genes exhibiting changes in gene expression during lens cell differentiation (Chi-square, $p < 1e\text{-}5$) also exhibited alterations in chromatin accessibility (50%) during lens cell differentiation relative to genes that did not exhibit changes in gene expression levels (26%). This data suggests that chromatin accessibility changes are significantly correlated with the differentiation state-specific expression levels of multiple genes during lens cell differentiation.

To further establish a relationship between changes in chromatin accessibility and changes in lens cell gene expression levels, we analyzed 2,549 of the 10,423 annotated genes that exhibited differential expression between at least two adjacent stages of lens cell differentiation (cutoff was |Log2 fold change FPKM| > 1, and false discovery rate adjusted p-value < 0.05) (Supplementary Table 2B). Of these genes, 508 genes were differentially expressed between undifferentiated lens epithelial cells (EC) and differentiating lens epithelial cells (EQ), 2,252 genes were differentially expressed between differentiating lens epithelial cells (EQ) and nascent lens fiber cells (FP), and 22 genes were differentially expressed between nascent lens fiber cells (FP) and terminally differentiated lens fiber cells (FC) (Fig. 4B). We then calculated the percentage of genes in each group that had a high Pearson correlation coefficient ($r > 0.7$) between chromatin accessibility changes proximal to the transcription start site (−7.5kbp/+2.5kbp of the TSS) and changes in gene expression level (Fig. 4B). We found that 36% of differentially expressed genes between EC and EQ, 52% of differentially expressed genes between EQ and FP, and 27% of differentially expressed genes between FP and FC were highly correlated ($r > 0.7$) with chromatin accessibility changes throughout progressive stages of lens cell differentiation (Fig. 4B). Chi-square analysis between differentiation-stage transitions (EC-EQ, EQ-FP, and FP-FC) and proportion of genes with highly correlated chromatin accessibility profiles revealed a statistically significant ($p < 1e\text{-}5$) relationship. This analysis revealed that the percentage of genes exhibiting both a positive correlation between chromatin accessibility and differentiation state-specific changes in gene expression was highest between the EQ-FP regions of the lens that make up the lens transition zone where epithelial cells are exiting the cell cycle and initiating their differentiation into lens fiber cells relative to other stages of lens cell differentiation.

To identify potential lens functions that could be regulated by alterations in chromatin accessibility, we performed functional gene clustering analysis on genes exhibiting a positive correlation between chromatin accessibility changes and gene expression levels at specific stages of lens differentiation (Fig. 4C) Comparisons were made between undifferentiated lens epithelium (EC) and differentiating lens epithelial cells of equatorial epithelium (EQ) (184 genes) and between equatorial epithelium (EQ) and nascent lens fiber cells (FP) (1183 genes) using the functional gene clustering tool from Pantherdb that enriches for statistically overrepresented biological processes (FDR corrected p-value < 0.05). The analysis revealed a number of critical lens processes that could be regulated by alterations in chromatin accessibility. In the EQ, cells must migrate from the anterior-most to posterior-most aspects of this region as they first withdraw from the cell cycle (Shi et al., 2015), initiate their differentiation program and begin to elongate. Pathways

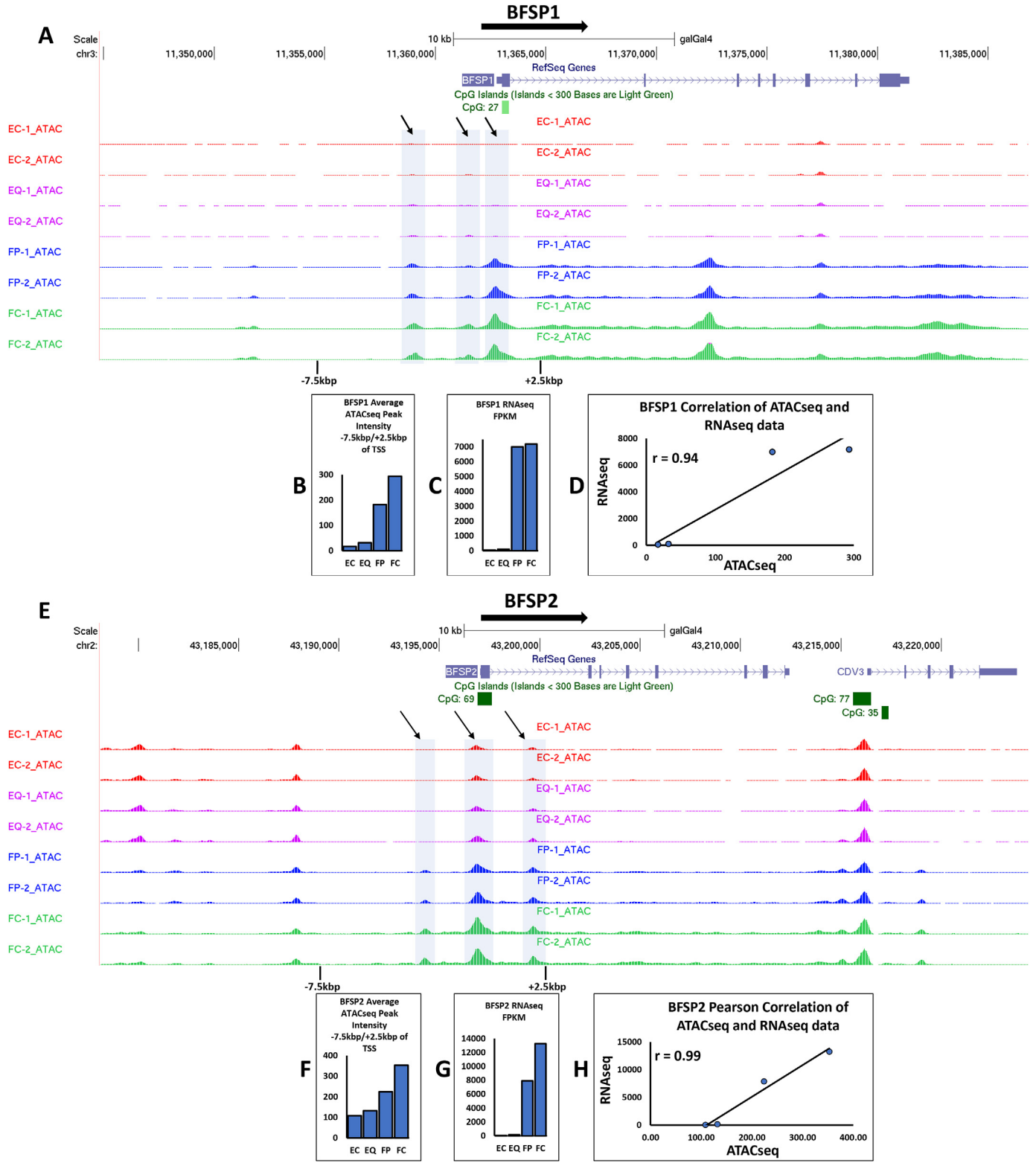

Fig. 3. Differentiation state-specific expression patterns of key lens genes correlate with changes in chromatin accessibility in potential gene regulatory regions. A. Chromatin accessibility map of the lens structural gene filensin (BFSP1) during progressive stages of lens cell differentiation (Red-EC, Violet-EQ, Blue-FP, Green-FC). Highlights and arrows indicate regions of altered chromatin accessibility within −7.5kbp/+2.5kbp of the transcription start site (TSS). B. The average peak intensity of chromatin accessible peaks within −7.5kbp/+2.5kbp of the TSS of BFSP1 across progressive stages of lens cell differentiation. Peak intensity data is provided by the ATACseq analysis. C. The corresponding gene expression profile of BFSP1 during progressive stages of lens cell differentiation. Gene expression data is taken from RNAseq analysis and quantified as FPKM. D. Plot of BFSP1 transcript FPKM vs Average peak intensity within −7.5kbp/+2.5kbp of the TSS of BFSP1 across the four progressive stages of lens differentiation. Data was correlated via Pearson correlation coefficient and is included in the plot. The same analysis was performed on the lens structural gene CP49 (BFSP2, E-H), the lens crystallin gene gamma-crystallin (CRYGN, I-L), the lens transcription factor paired box 6 (PAX6, M-P), and the lens cystallin gene delta-cystallin (ASL1, Q-T).

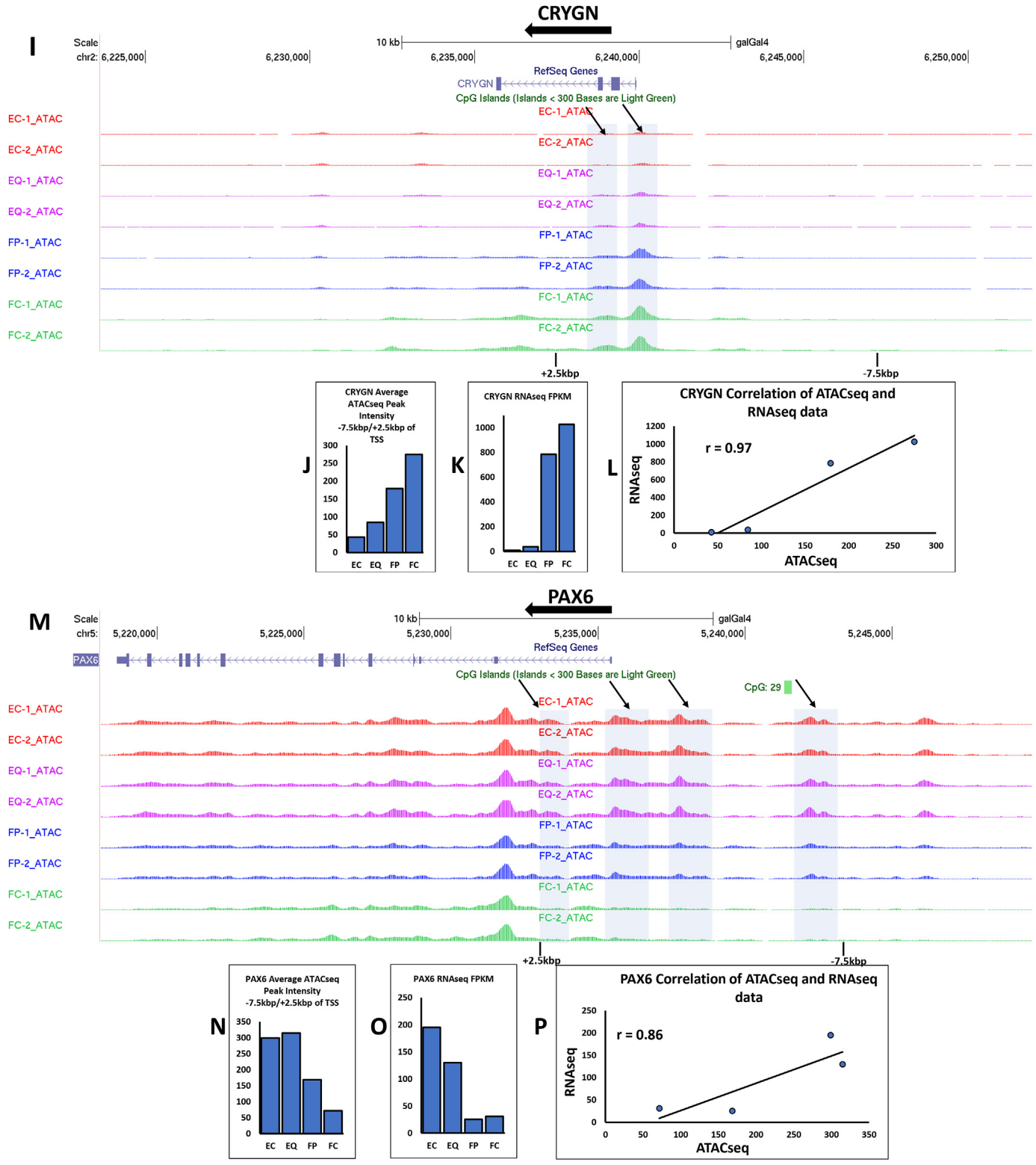

Fig. 3. (*continued*).

associated with this process included the Wnt signaling pathway, which has been linked to the maintenance of planar cell polarity of the cells in the EQ (Chen et al., 2008) and the early stages of lens differentiation that occur in this zone (Martinez et al., 2009; Stump et al., 2003). Analysis of the transition from equatorial epithelium (EQ) to the highly elongated lens fiber cells of the FP region (FP) reveals many biological processes linked in general to cell differentiation and development, as well as a particularly high concentration of processes linked to cell morphogenesis. This morphogenetic process requires growth factor signaling, especially pathways activated by FGF (Lovicu et al., 2011; Lovicu and McAvoy, 2005). Our analysis shows transition to the FP zone involves upregulation of genes associated with the cellular response to growth factor stimulus and signaling through serine/threonine kinases that function as their downstream effectors. Together, this analysis suggests

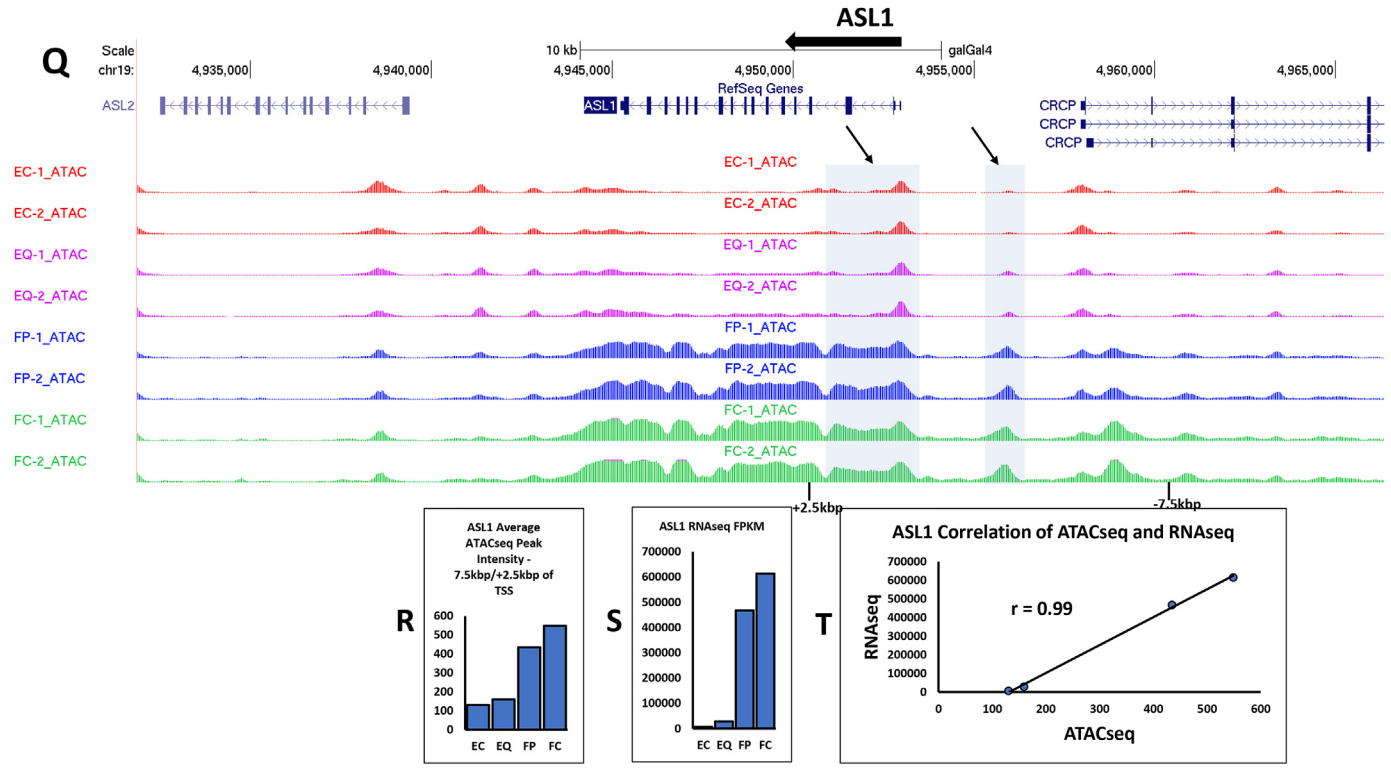

Fig. 3. (*continued*).

that changes in chromatin accessibility may be crucial for regulating the expression levels of multiple genes important for a wide-range of key biological processes at distinct stages of lens differentiation.

The relationship between chromatin accessibility and changes in gene expression during lens cell differentiation (cutoff was |Log2 fold change FPKM| > 1, and false discovery rate adjusted p-value < 0.05) was also analyzed for 189 genes with established lens functions. Relative gene expression levels for these genes are shown as Morpheus plots (Fig. 5A, C, E, G) with increased gene expression levels shown as red and decreased levels shown as blue. Chromatin accessibility changes were quantified at the region proximal to the transcription start site (−7.5kbp/+2.5kbp of the TSS) and the region proximal to the gene body (±10kbp of their gene bodies) as described in methods. Chromatin accessibility changes at the region proximal to the transcription start site and also the region proximal to the gene body were each correlated with gene expression levels of the 189 genes via Pearsons correlation analysis (Fig. 5B, D, F, H). 91 genes with known lens functions were found to have a high correlation (r > 0.7) between altered chromatin accessibility at the region proximal to their transcriptional start sites and their differentiation state-specific gene expression levels. 94 genes with known lens functions were found to have a high correlation (r > 0.7) between altered chromatin accessibility at the region proximal to their gene bodies and their differentiation state-specific gene expression levels. 73 genes with known lens functions were found to have a high correlation (r > 0.7) between differentiation state-specific gene expression levels and altered chromatin accessibility at both the region proximal to their transcriptional start sites and the region proximal to their gene bodies.

The identified lens genes exhibiting a high correlation with chromatin accessibility changes and gene expression levels have a multitude of important cellular functions and included those required for lens cytoskeletal structure (BFSP1, BFSP2) (Perng et al., 2007), gap junctions (GJA1) (Beyer and Berthoud, 2014), post-transcriptional control (TDRD7) (Lachke et al., 2011), lens refractive index regulation (EPHA2) (Shi et al., 2012), lens crystallins (CRYBB1, CRYBA4, ASL1, CRYGN, CRYGS, CRYL1) (Wistow, 2012), transcription factors (HSF4 (Gao et al., 2017), SMAD3 (Meng et al., 2018), HIF1A (Shui et al., 2008a), SOX2 (Smith et al., 2009)), autophagy regulation and lysosomal transport (FYCO1) (Chen et al., 2011), notch-signaling regulation (NOTCH1, HES5 (Jia et al., 2007; Rowan et al., 2008)) and Wnt-signaling regulation (WNT5a, WNT2B, WNT7B, LGR4, LGR5, CER1 (Stump et al., 2003)). The analysis suggests that multiple cellular functions including those previously established to be important for lens regulation, homeostasis and structure may be dependent on gene regulation controlled by alterations in chromatin accessibility in potential DNA regulatory regions.

3.3. *Multiple transcription factor binding consensus sequences are contained within regions of altered chromatin accessibility*

The above analysis identified 73 genes with established important lens functions that exhibited high Pearson correlations (r > 0.7) between altered levels of gene expression and chromatin accessibility changes during lens cell differentiation. Since the differences in chromatin accessibility could point to transcription factor binding sequences specific for transcription factors that could be regulated at least in-part through chromatin regulated access to their DNA binding sites, we analyzed the identified regions of altered chromatin accessibility in potential promoter (−7.5kb/+2.5kbp to the start of transcription) and ± 10 kb of the gene body regions of the 73 genes for specific transcription factor binding consensus sequences using the AME tool (MEME-suite 5.0.3) as described in methods.

The analysis revealed a wide variety of transcription factor binding motifs in these DNA regions including consensus sequences for members of the nuclear factor of activated T-cells family of transcription factors (NFATs), the forkhead box family of transcription factors (FOXs), and among others HIF1A, IRF1, RBPJ, SP2 and TEAD1 (Fig. 6A). Analysis of the corresponding gene expression profiles of these transcription factors revealed multiple differences in their expression patterns during lens cell differentiation (Fig. 6B). Detailed analysis of predicted transcription factor binding sites for several key lens genes are shown in Fig. 6C–G. Genomic positions of potential transcription factor binding sites relative

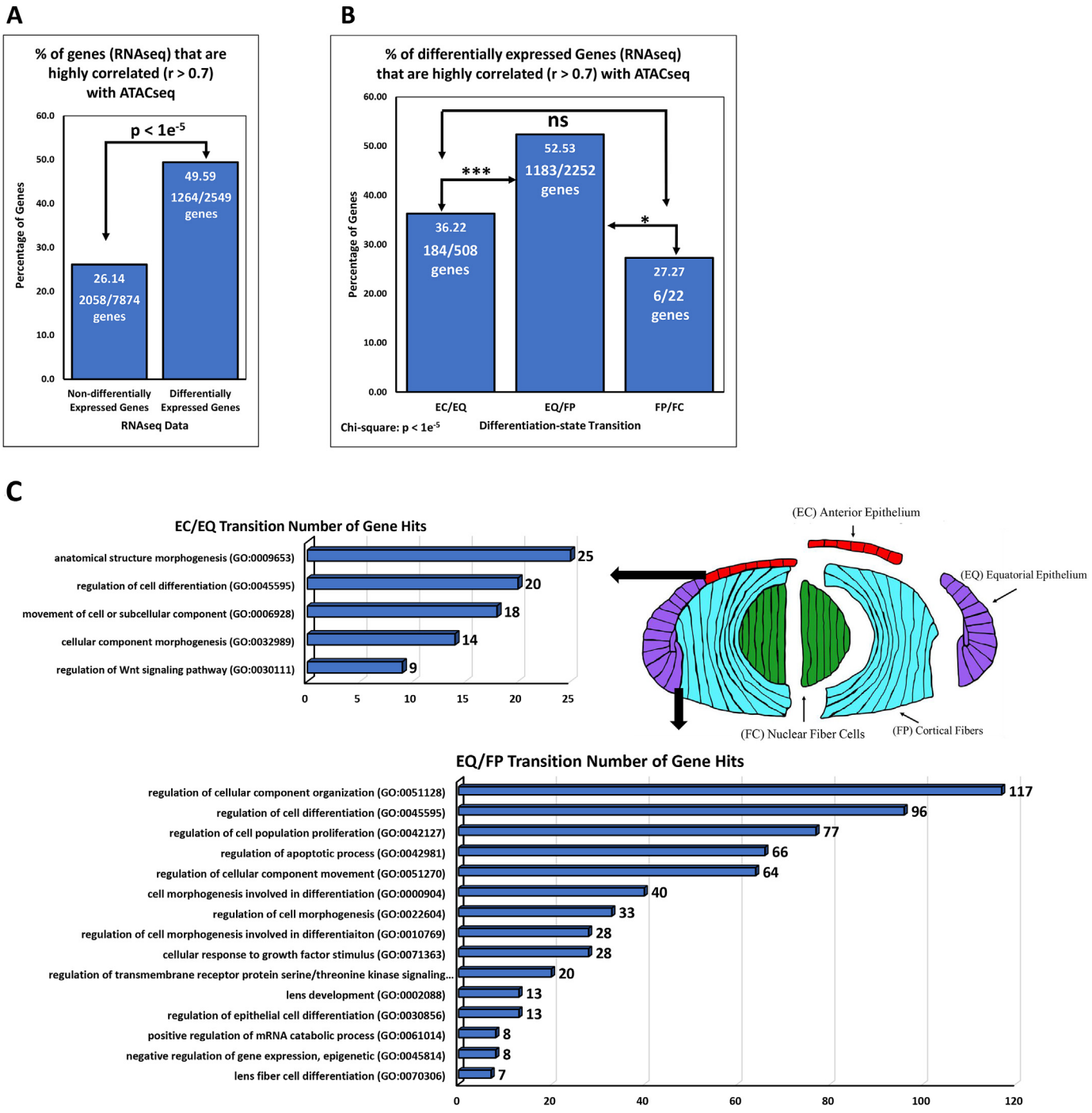

Fig. 4. Differentiation state-specific expression patterns of multiple genes are highly correlated with chromatin accessibility changes in potential DNA regulatory regions. A. Barplot showing the percentage of differentially expressed genes (|Log2 fold change FPKM| >1 between any two adjacent stages of lens cell differentiation, and adj p-value < 0.05) that are highly correlated (r > 0.7) with chromatin accessibility changes proximal to the transcription start site (within −7.5kbp/+2.5kbp of the TSS). Chi-squared analysis was performed to compare the result to the percentage of non-differentially expressed genes (|Log2 fold change FPKM <1|, and/or adj-p-value > 0.05) that were highly correlated with chromatin accessibility changes proximal to the transcription start site. B. Barplot showing the percentage of differentially expressed genes at each stepwise comparison (EC/EQ, EQ/FP, FP/FC) that are highly correlated (r > 0.7) with chromatin accessibility changes proximal to the transcription start site. Chi-squared analysis was performed to compare the results of each stepwise comparison to each other. ***p < 0.001, *p<0.05, ns p>0.05. C. 1373 genes with a high pearson correlation (r > 0.7) between chromatin accessibility changes and statistically significant gene expression changes between progressive stages of lens cell differentiation (EC/EQ, EQ/FP, FP/FC) were analyzed for statistical overrepresentation of key Biological Processes associated with these genes. This gene enrichment analysis revealed 5 overrepresented biological processes associated with the genes differentially expressed between quiescent epithelial cells (EC) and differentiating epithelial cells (EQ), 15 overrepresented biological processes associated with the genes differentially expressed between differentiating epithelial cells (EQ) and nascent lens fiber cells (FP), 0 overrepresented biological process associated with the genes differentially expressed between nascent lens fiber cells (FP) and terminally differentiated lens fiber cells (FC).

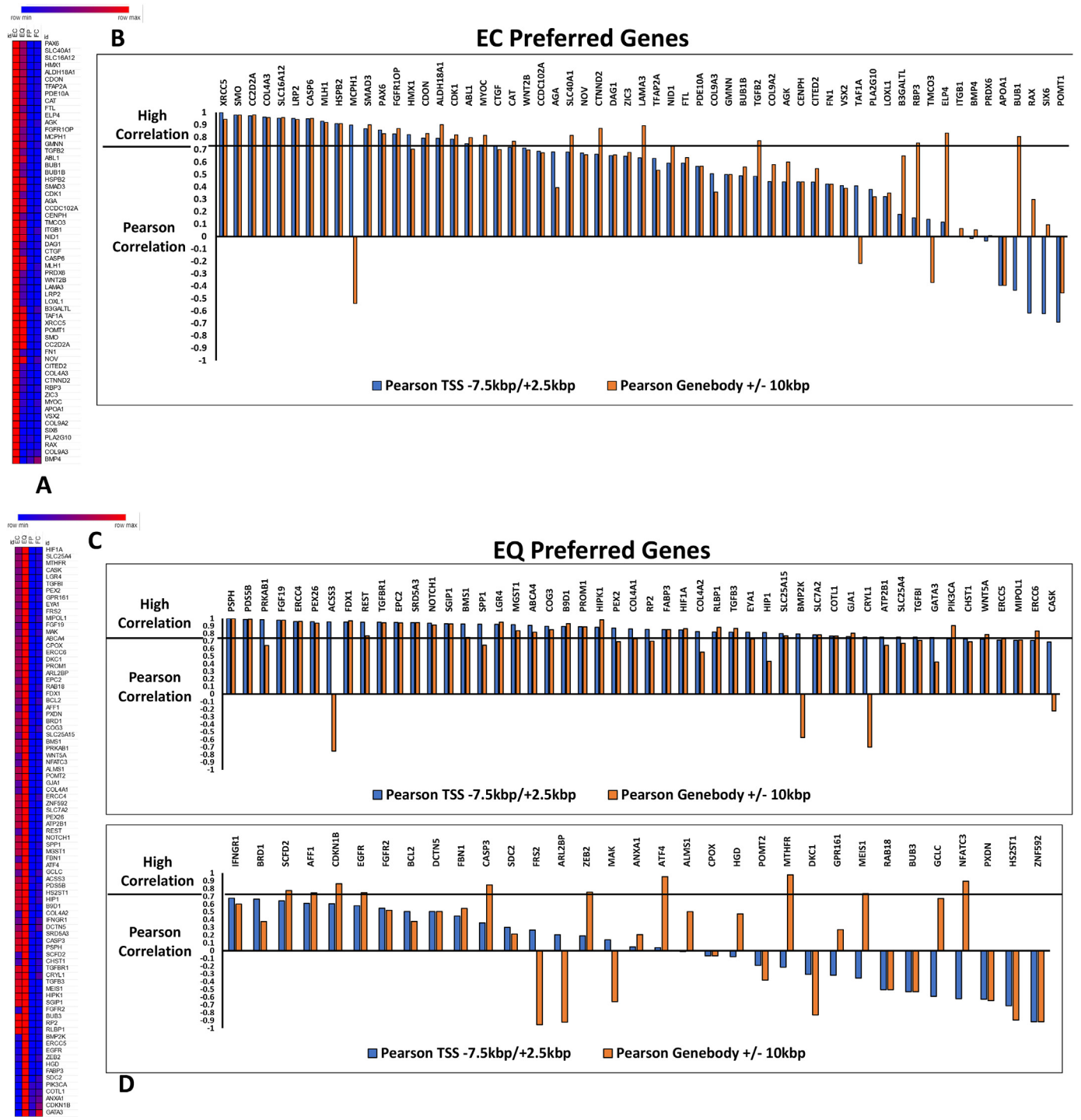

Fig. 5. Expression patterns of important lens genes correlate with chromatin accessibility changes in potential DNA regulatory regions. A. Morpheus heatmaps demonstrating expression profiles of specific lens genes most highly expressed in quiescent lens epithelial cells (EC, quantified by FPKM from RNAseq) across the four stages of lens differentiation (red high expression, blue low expression). B. Barplots showing pearson correlation coefficient values calculated between average peak intensity of chromatin accessibility regions proximal to the transcription start site (dark blue) and proximal to the gene body (orange) of these specific lens genes compared to their gene expression profiles. The same analysis was performed for specific lens genes most highly expressed in differentiating lens epithelial cells (EQ, C-D), nascent lens fiber cells (FP, E-F), and terminally differentiated lens fiber cells (FC, G-H).

to the transcription start site of their respective genes are labeled. Only potential sites with $p < 1e\text{-}4$ are reported and only one site per transcription factor per gene is included. The gamma crystallin gene CRYGN exhibits increasing chromatin accessibility defined by increasing peak intensities at the two highlighted regions (Fig. 6C). Potential binding sites for the transcription factors RBPJ, SPIC, and CTCF are found proximally upstream to the transcription start site (TSS), and a potential binding site for the transcription factor MYOD1 was found in the gene body at a potential enhancer region. The lens structural gene BFSP1 exhibits increasing chromatin accessibility defined by increasing peak intensities at the three highlighted regions (Fig. 6D). Potential binding sites for the transcription factors CTCF, SPIC, and MEF2C are found upstream

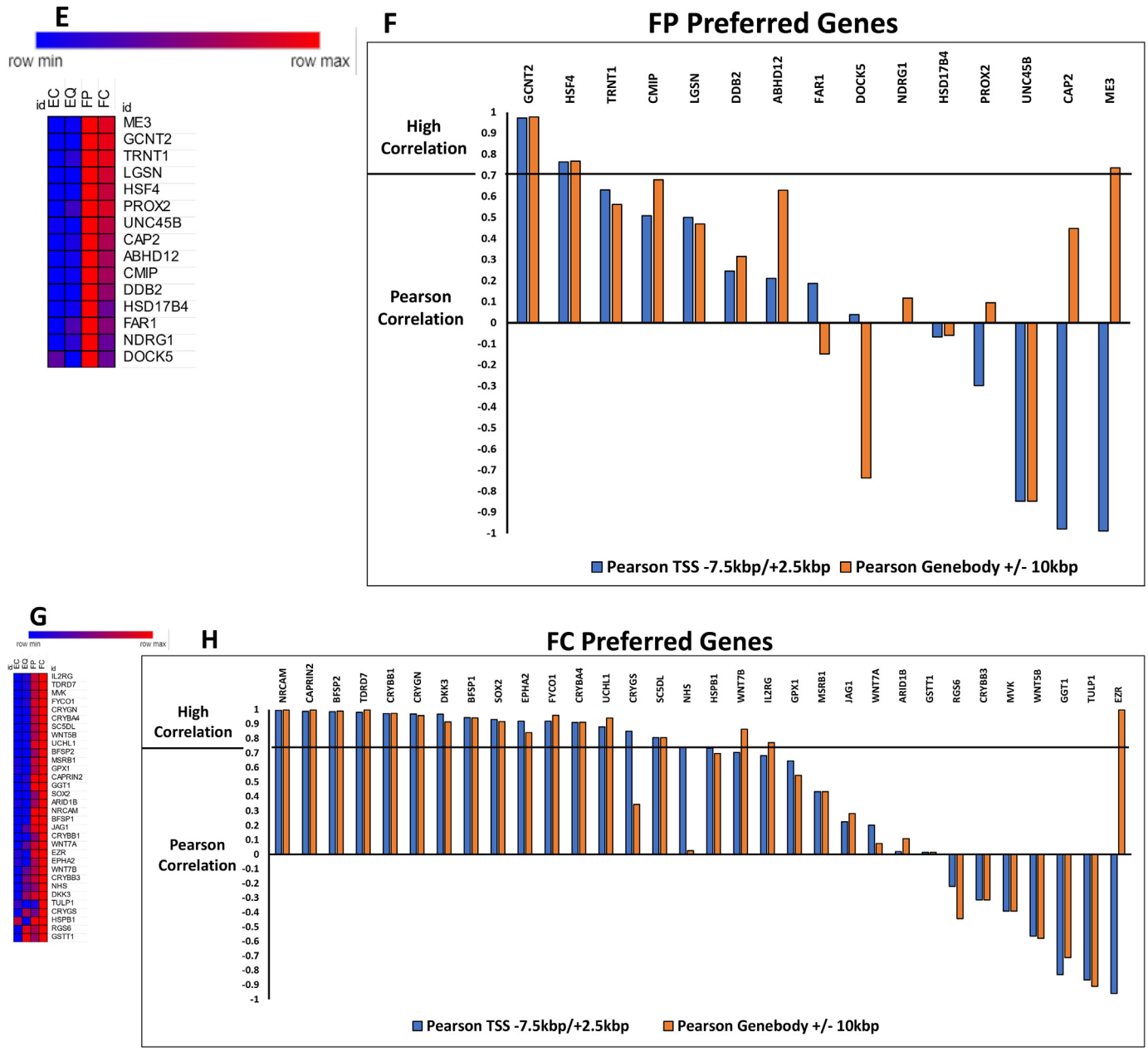

Fig. 5. (*continued*).

to the TSS, potential sites for SP2 and MYOD1 are found proximally downstream of the TSS, and a potential site for TEAD1 was found in the gene body at a potential enhancer region. Similar analysis was also performed for the lens structural gene BFSP2, the lens transcription factor PAX6, the lens cell membrane protein of the notch signaling pathway NOTCH1, and the delta crytallin gene ASL1.

Interestingly, the majority of these transcription factors have not yet been studied in the lens and this analysis suggests they may play an important role in regulating the expression of these genes during lens cell differentiation. Consistently, other transcription factors identified in this analysis have established functions in the differentiation and/or development of the lens and other tissues. For instance, NFATs (Horsley and Pavlath, 2002; Serrano-Pérez et al., 2015; Wang et al., 2011) and the forkhead box family of transcription factors (Tuteja and Kaestner, 2007a, 2007b) have been widely studied for their roles in epithelial cell differentiation in non-lens tissues. Lens-specific conditional knockout of FOXP1 in mice resulted in normal lens development, however, the mature lenses of the FOXP1 conditional knock-out mice exhibit disrupted fiber cell structure, suggesting an important function for FOXP1 in lens cell differentiation (Suzuki-Kerr et al., 2017). Similarly, lens specific conditional HIF1 knockout mice exhibit normal lens development but their lenses disintegrate shortly after birth suggesting altered differentiation in these mice (Shui et al., 2008b). Lens-conditional knockout of the Notch signaling effector RBPJ provided evidence that RBPJ regulates growth and differentiation of the lens though regulation of key cell cycle control pathways (Rowan et al., 2008). Interestingly, ARID3B which is both a transcription factor (Fig. 6A) and chromatin modifier (Fig. 7) has been predicted to regulate fiber cell differentiation through bioinformatics analysis of transcription factors whose expression is enriched in the epithelium and fiber cells of the mouse lens (Zhao et al., 2018b). Collectively, these data provide evidence that the identified alterations in chromatin accessibility could regulate the binding and function of multiple transcription factors that likely coordinate the expression of a wide-variety of genes during lens cell differentiation.

A

Transcription Factors	E-value	% of sequences	Sequence Binding Motifs
NFATC2	3E-19	48	
IRF1	8E-18	25	
NFAT5	2E-17	55	
ZNF384	3E-15	9	
FOXP2	4E-13	27	
CTCF	5E-12	9	
FOXK1	3E-10	31	
FOXP1	9E-10	37	
FOXK2	1E-09	36	
Arid3b	3E-08	36	
NFATC3	3E-07	46	
RBPJ	3E-07	20	
E2F6	5E-07	24	
SP2	5E-07	15	
NFATC1	3E-06	38	
ARNT::HIF1A	5E-06	26	
Hoxd9	7E-06	47	
FOXO4	6E-05	34	
Foxj2	1E-03	34	
MEF2C	1E-03	18	
Myod1	1E-03	7	
TEAD1	5E-03	19	
SPIC	1E-02	18	
FOXI1	1E-02	17	
FOXB1	4E-02	9	

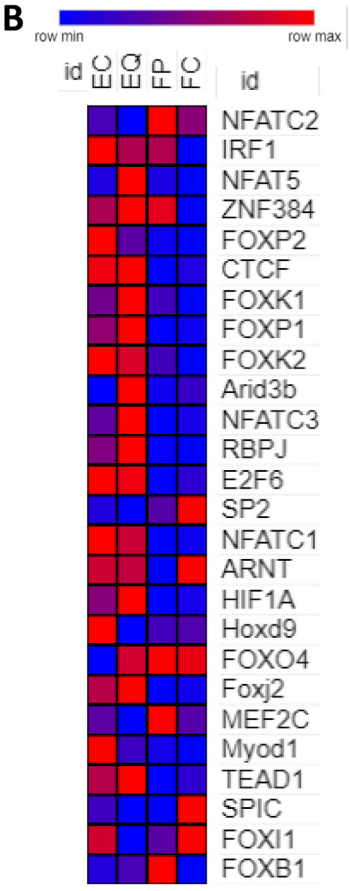

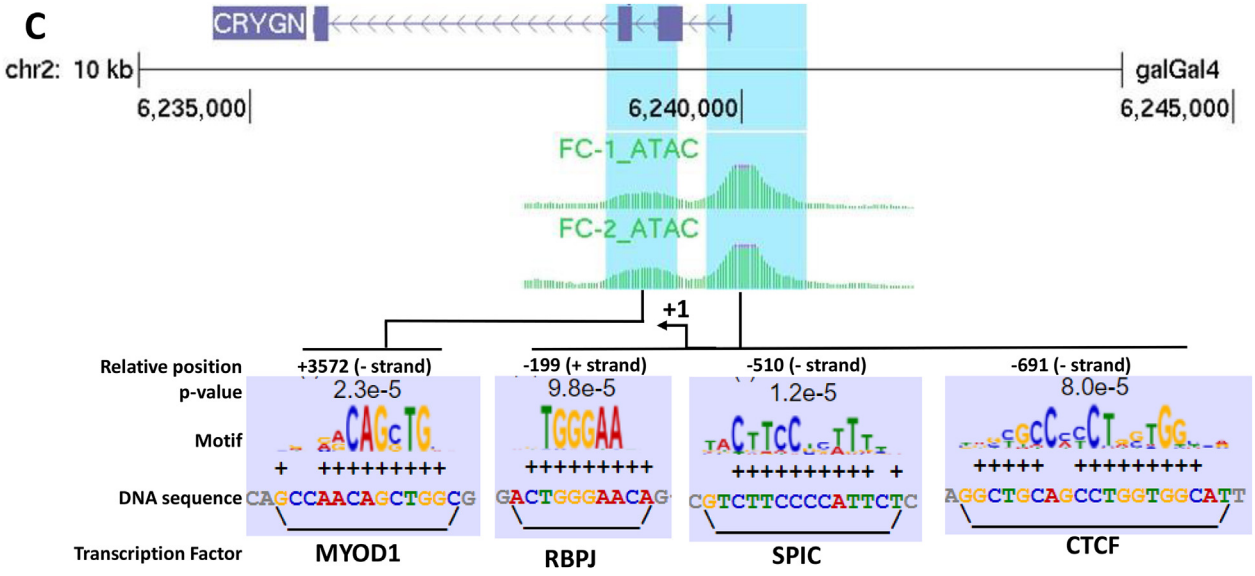

Fig. 6. Multiple transcription factor binding sites are located in regions of altered chromatin accessibility in potential DNA regulatory regions of important lens genes. A. The chromatin accessibility profiles proximal to the TSS (−7.5kbp/+2.5kbp) and Genebodies (±10 kbp) of 73 genes with associated lens functions were highly correlated with their respective gene expression profiles across the four stages of lens differentiation (Fig. 5). Analysis of chromatin accessible regions of these genes (AME tool MEME-suite 5.0.3) revealed 25 transcription factor binding motifs with high statistically significant representation (E-value < 0.05) in the chromatin accessible regions of these genes. The E-value, percent of sequences containing the motif, and the consensus binding sequences are listed. B. Morpheus heatmaps demonstrating expression profiles of these 25 transcription factors (quantified by FPKM from RNAseq) across the four stages of lens differentiation (red is high expression, blue is low expression). C. Chromatin accessibility map of the lens crystallin gene crystallin gamma-N (CRYGN) during progressive stages of lens cell differentiation. Blue highlights indicate regions of chromatin accessibility that contain the detected transcription factor binding sites. Also labeled are the relative positions of the most statistically significant transcription factor binding sites detected in these chromatin accessible regions. Transcription factor binding motifs, corresponding DNA sequences, and p-values for each match are reported. The same analysis and depiction of transcription factor binding sites matched to the fiber cell structural proteins filensin (BFSP1) and CP49 (BFSP2) (D and E respectively), the lens transcription factor Paired Box 6 (PAX6, F), the transmembrane protein of the Notch signaling pathway (NOTCH1, G), and the lens crystallin gene delta crystallin (ASL1, H). For each gene ATACseq tracks representing the differentiation state specific region that each gene is most highly expressed in are shown to visualize regions of open chromatin containing the transcription factor binding motifs.

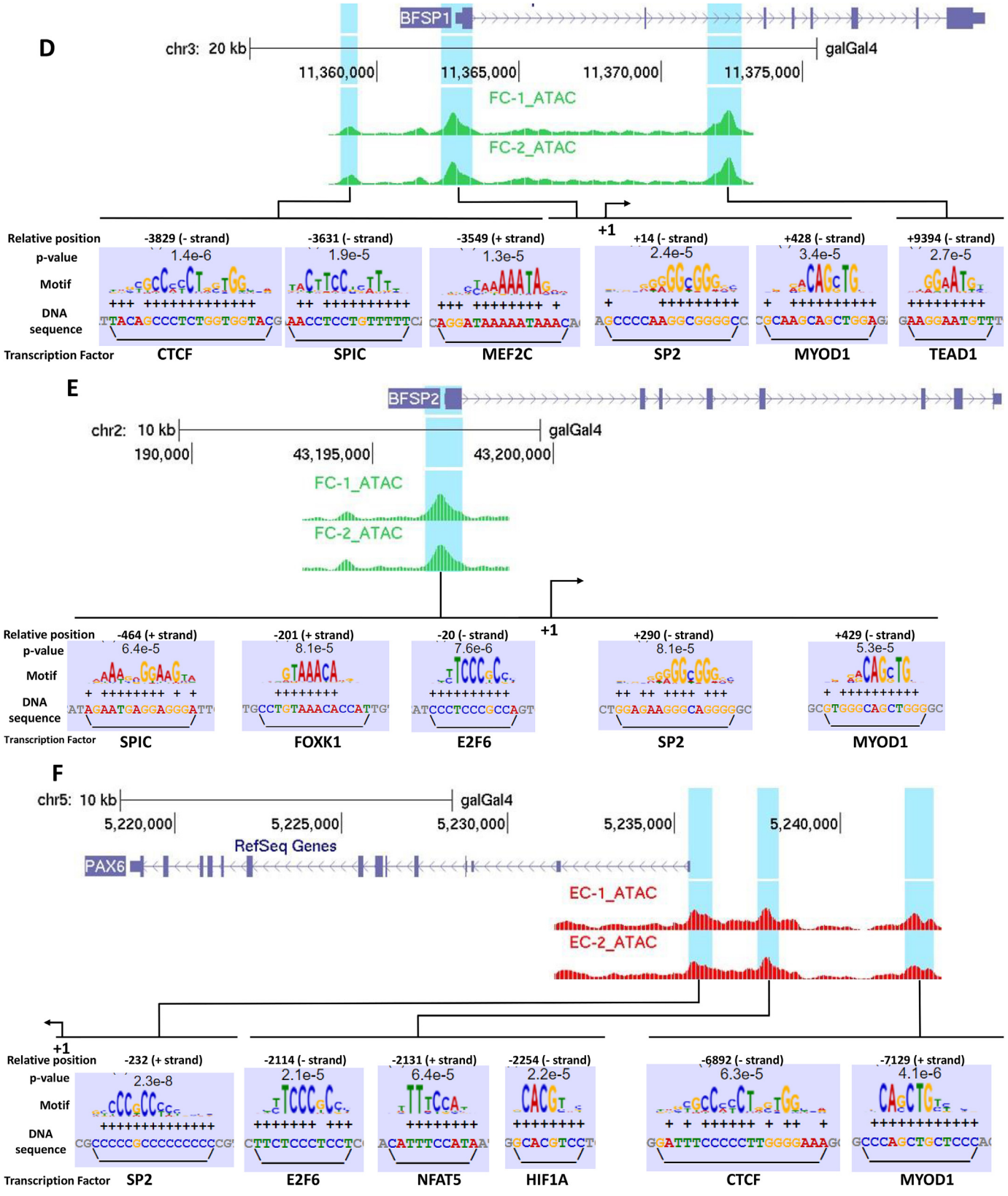

Fig. 6. (*continued*).

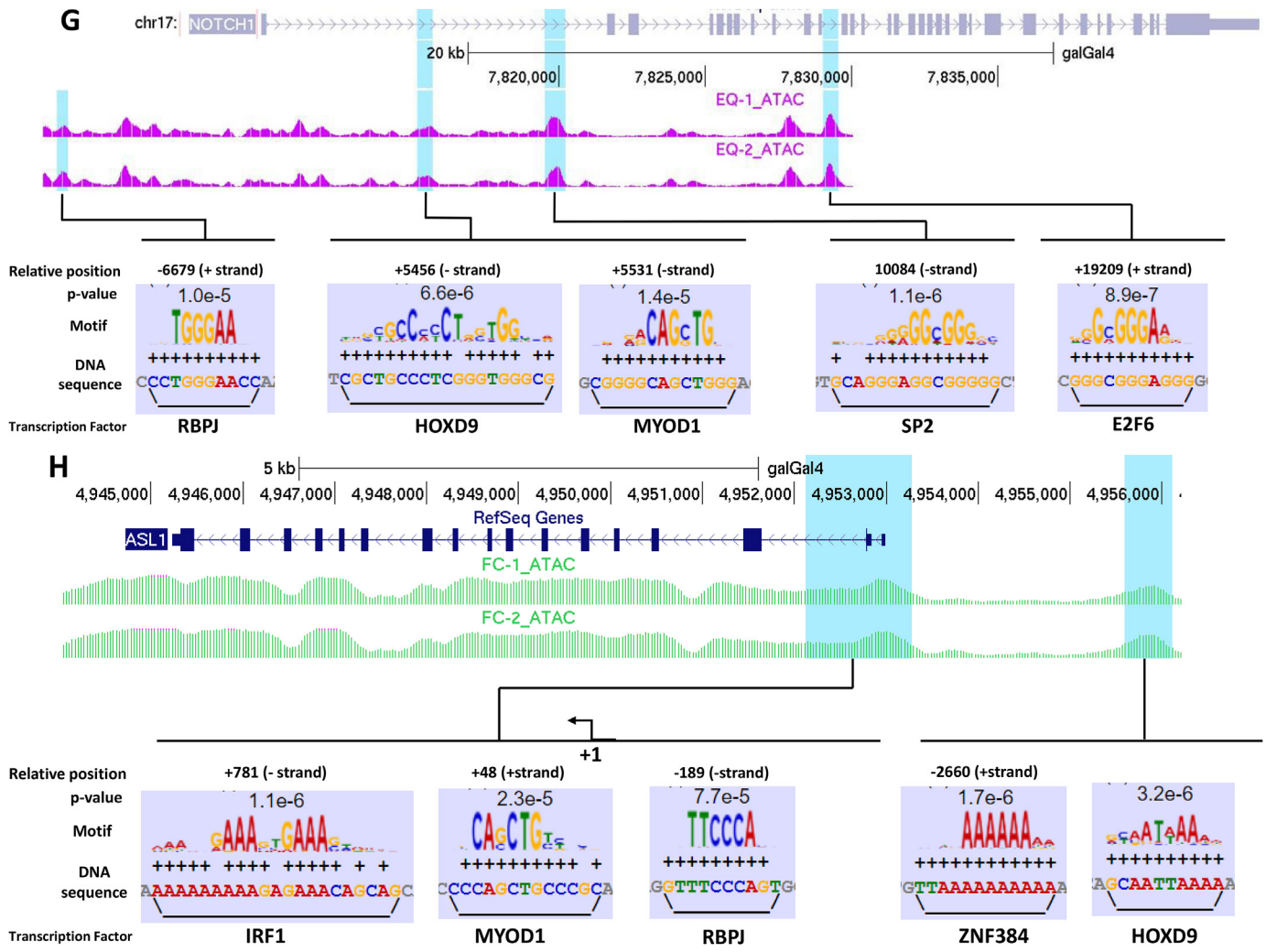

Fig. 6. (*continued*).

3.4. Chromatin modifying proteins exhibit asymmetric expression levels during lens cell differentiation

At present, the mechanism(s) underlying the detected changes in chromatin accessibility remain to be identified. However, a previous study established a relationship between the levels of the chromatin remodeling enzyme Snf2h (SMARCA5) and lens development (He et al., 2016). To identify additional chromatin remodeling enzymes that could coordinate the changes in chromatin accessibility detected in the present study, we interogated our RNA sequencing for the expression patterns of over 60 genes implicated in chromatin remodeling or modification. Our analysis identified that genes encoding a wide range of chromatin remodeling enzymes and DNA modification proteins exhibited altered expression during lens differentiation (Fig. 7). Analysis of their expression patterns revealed that a large number exhibit lens cell differentiation-state specific expression patterns. These include CITED2, and HDAC1 that are mainly expressed in undifferentiated epithelial cells (EC); SMARCA2, SMARCA5, and ARID3B that are mainly expressed in the transition zone of the lens where epithelial cells are proliferating and exiting the cell cycle to initiate differentiation (EQ); CHD2, and CHD1L that are mainly expressed in nascent lens fiber cells undergoing cellular elongation (FP); and BRD4, ARID3A, and BAZ2A that are mainly expressed in terminally differentiated lens fiber cells (FC). Interestingly, the majority of the differentiation specific expression patterns of these genes, in particular the SWI/SNF family and ARID family, are detected in EQ where lens differentiation is initiated and cellular remodeling begins suggesting a critical role for these proteins in this key stage of lens cell differentiation.

4. Discussion

A key component towards advancing fields ranging from regenerative medicine to cancer therapy is the identification of novel pathways driving cellular differentiation. A well-studied model system is the lens that is composed of easily isolatable cell populations in distinct stages of cellular differentiation. These cell populations include a monolayer of quiescent cuboidal epithelial cells at the lens anterior, a monolayer of replicative epithelial cells at the lens equator that withdraw from the cell cycle to initiate differentiation, a zone of newly formed fiber cells at the lens cortex that undergo a series of remodeling events including elongation and, a central core of elongated fiber cells that lose their organelles as they undergo terminal differentiation and make up the bulk of the lens (Bassnett et al., 2011; Menko, 2002; Piatigorsky, 1981; Audette et al., 2017; Chauss et al., 2014; Cheng et al., 2017; Costello et al., 2013; FitzGerald, 2009; Mathias et al., 2010; Perng et al., 2007; Rao and Maddala, 2006; Robinson, 2006; Lovicu and McAvoy, 2005; Brennan et al., 2018).

Although previous studies have identified multiple requirements for lens cell differentiation including the essential roles of growth factors (Lovicu and McAvoy, 2005; Robinson et al., 1995; Xu et al., 1998), integrins (Walker et al., 2002) and transcription factor-mediated signaling pathways (Rowan et al., 2008; Song et al., 2014; Stump

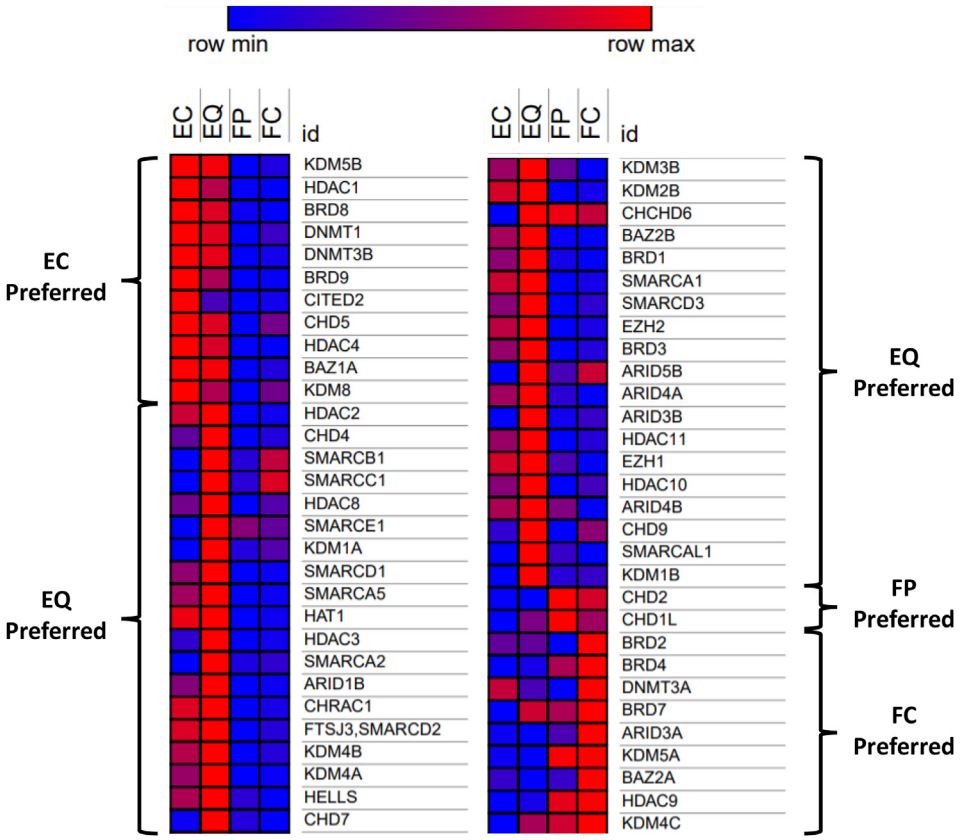

Fig. 7. Expression patterns of selected chromatin modifying proteins at distinct stages of lens cell differentiation. Morpheus heatmaps demonstrating expression profiles of genes encoding chromatin remodeling enzymes and DNA modification proteins (quantified by FPKM from RNAseq) across the four stages of lens differentiation (red high expression, blue low expression). The genes are sorted by the differentiation state-specific region each gene is most highly expressed in.

et al., 2003), the potential role for chromatin accessibility in the regulation of lens cell differentiation has not been previously examined. Here, we examined the genome-wide changes in chromatin accessibility specific for four distinct stages of lens differentiation, we correlated the identified changes in chromatin accessibility with the differentiation stage-specific expression profiles of over 10,000 genes and we mapped the potential DNA regulatory sequences and transcription factor binding sequences that could control their differentiation state-specific expression patterns.

Our analysis identified 89,904 regions of chromatin accessibility correlating with distinct stages of lens cell differentiation. Although the data do not establish a direct cause and effect relationship between altered chromatin accessibility and lens cell differentiation, the data do establish that changes in chromatin accessibility are a major feature of lens differentiation and they demonstrate that specific changes in chromatin accessibility parallel a wide-range of differentiation state-specific gene expression patterns. Although multiple normalization procedures were employed in our analysis to eliminate possible differences in chromatin accessibility at specific sites arising as a consequence of differences in cell number between samples, we cannot entirely rule out this potential effect on individual changes in chromatin accessibility detected. Consistent with chromatin accessibility changes being specific for distinct stages of the lens cell differentiation program, the bulk of specific chromatin accessibility changes were detected in the transition zone of the lens where lens epithelial cells are dividing, exiting the cell-cycle, and initiating their differentiation program.

Our results are also in line with previous studies linking chromatin accessibility changes to cell-type specificity in non-lens cells. For instance, differences in chromatin accessibility were detected between terminally differentiated pancreatic alpha and beta and acinar cells (Ackermann et al., 2016) and another study that reported differences in chromatin accessibility between specific myeloid lineages at distinct stages of differentiation in an artificially induced cell culture model (Ramirez et al., 2017). Finally, genome wide-chromatin accessibility profiles have also been established for differentiating CD8 T-cell populations isolated from different aged-donors (Moskowitz et al., 2017).

The specific changes in chromatin accessibility identified in the present report suggest that changes in chromatin accessibility could be important for regulating key trends in gene expression levels specific for distinct stages of the lens cell differentiation program. Consistent with this possibility, 50% of genes whose expression levels are distinct for one or more stages of lens cell differentiation displayed high correlations ($r > 0.7$) with chromatin accessibility changes. Consistent with the possibility that changes in chromatin accessibility contribute towards regulating the function of these genes, over 73 genes with established important lens functions exhibited a high correlation ($r > 0.7$) between specific changes in chromatin accessibility and their mRNA expression levels during lens differentiation.

Lens genes exhibiting a high correlation between chromatin accessibility changes and gene expression levels have a multitude of important cellular functions. These genes included those required for lens cytoskeletal structure (BFSP1, BFSP2) (Perng et al., 2007), gap junctions (GJA1) (Beyer and Berthoud, 2014), post-transcriptional control (TDRD7) (Lachke et al., 2011), lens refractive index regulation (EPHA2) (Shi et al., 2012), lens crystallins (CRYBB1, CRYBA4, ASL1, CRYGN, CRYGS, CRYL1) (Wistow, 2012), transcription factors (HSF4 (Gao et al., 2017), SMAD3 (Meng et al., 2018), HIF1A (Shui et al., 2008a), SOX2 (Smith et al., 2009)), autophagy regulation and lysosomal transport (FYCO1) (Chen et al., 2011), notch-signaling regulation (NOTCH1, HES5 (Jia et al., 2007; Rowan et al., 2008)) and Wnt-signaling regulation (WNT5a, WNT2B, WNT7B, LGR4, LGR5, CER1 (Stump et al., 2003)).

Consistent with changes in chromatin accessibility being important for the differentiation state-specific expression of these genes, our results also indicate that the majority of chromatin accessibility changes correlating with differentiation state-specific gene expression are most abundant during the transition from lens epithelial cells to lens fiber cells in the lens transition zone. These chromatin accessibility changes are mainly found within −7.5 kb/+2.5kbp to the transcriptional start sites and/or between ± 10 kb from the gene body of the identified genes. Although further functional studies will be required to establish the regulatory importance of these regions for control of individual genes, the identified sequences nevertheless provide clues as to what chromatin-regulated DNA sequences are likely important for control of their expression patterns during lens cell differentiation. Analysis of sequences with altered chromatin accessibility at potential promoter (−7.5kb/+2.5kbp to the transcriptional start site) and potential cis-regulatory regions (within ± 10 kb from the gene body) of these genes identified a number of consensus transcription factor binding sequences that point to a number of transcription factors that could regulate the expression of these genes. These include potential binding sites for transcription factors for PAX6 (Cvekl and Zhang, 2017; Sun et al., 2015), TEAD1, the FOX family of transcription factors (Medina-Martinez and Jamrich, 2007), RBPJ, HIF1A (Shui et al., 2008a), and the NFAT family of transcription factors. Although these positive correlations implicate chromatin accessibility as a potential regulator of the binding of these transcription factors during lens differentiation, the galGal4 genome lacks well-established annotations for distinct promoters or other cis-acting regulatory regions, and lacking these annotations, we cannot rule out that more proximal or distal regions from the gene body could also be important for the regulation of these genes.

To date, the mechanisms regulating altered chromatin accessibility during lens cell differentiation are not known. However, our analysis of the expression patterns of multiple chromatin modifying proteins identified differences in their expression patterns at progressive stages of the lens cell differentiation program that could indicate differentiation state-specific functions including their playing important regulatory roles in governing the chromatin accessibility landscape at different stages of lens cell differentiation. Consistently, a previous study showed that deletion of the chromatin remodeling enzyme SNF2H resulted in altered embryonic lens differentiation in association with changes in the levels of PAX6, P27 and HSF4 (He et al., 2016).

In summary, the present data implicate changes in chromatin accessibility as an essential feature of lens cell differentiation and they identify a wide-variety of lens genes whose altered expression during lens differentiation is likely regulated by changes in chromatin accessibility. The data also identify specific DNA sequences and transcription factors that could be critical for regulating the differentiation state-specific expression patterns of multiple important lens genes and they point to chromatin modifying proteins that could be important for remodeling the chromatin landscape at distinct stages of the lens cell differentiation program. The findings provide the basis for future experiments to further establish the role of chromatin accessibility in the control of lens cell differentiation and they provide a blueprint for understanding the potential role for chromatin accessibility in the differentiation and function of more complex tissues.

Appendix A. Supplementary data

Supplementary data to this article can be found online at https://doi.org/10.1016/j.ydbio.2019.04.020.

References

Ackermann, A.M., Wang, Z., Schug, J., Naji, A., Kaestner, K.H., 2016. Integration of ATAC-seq and RNA-seq identifies human alpha cell and beta cell signature genes. Mol. Metab. 5, 233–244. https://doi.org/10.1016/j.molmet.2016.01.002.

Audette, D.S., Scheiblin, D.A., Duncan, M.K., 2017. The molecular mechanisms underlying lens fiber elongation. Exp. Eye Res. 156, 41–49. https://doi.org/10.1016/j.exer.2016.03.016.

Bailey, T.L., Boden, M., Buske, F.A., Frith, M., Grant, C.E., Clementi, L., Ren, J., Li, W.W., Noble, W.S., 2009. MEME SUITE: tools for motif discovery and searching. Nucleic Acids Res. 37, W202–W208. https://doi.org/10.1093/nar/gkp335.

Bailey, T.L., Gribskov, M., 1998. Combining evidence using p-values: application to sequence homology searches. Bioinformatics 14, 48–54. https://doi.org/10.1093/bioinformatics/14.1.48.

Bassnett, S., Shi, Y., Vrensen, G.F.J.M., 2011. Biological glass: structural determinants of eye lens transparency. Philos. Trans. R. Soc. Lond. B. Biol. Sci. 366, 1250–1264. https://doi.org/10.1098/rstb.2010.0302.

Beyer, E.C., Berthoud, V.M., 2014. Connexin hemichannels in the lens. Front. Physiol. 5, 20. https://doi.org/10.3389/fphys.2014.00020.

Brennan, L.A., McGreal-Estrada, R., Logan, C.M., Cvekl, A., Menko, A.S., Kantorow, M., 2018. BNIP3L/NIX is required for elimination of mitochondria, endoplasmic reticulum and Golgi apparatus during eye lens organelle-free zone formation. Exp. Eye Res. 174, 173–184. https://doi.org/10.1016/j.exer.2018.06.003.

Buenrostro, J.D., Giresi, P.G., Zaba, L.C., Chang, H.Y., Greenleaf, W.J., 2013. Transposition of native chromatin for fast and sensitive epigenomic profiling of open chromatin, DNA-binding proteins and nucleosome position. Nat. Methods 10, 1213–1218. https://doi.org/10.1038/nmeth.2688.

Chandler, L.A., Jones, P.A., 1988. Hypomethylation of DNA in the regulation of gene expression. Dev. Biol. (N. Y. 1985) 5, 335–349.

Chauss, D., Basu, S., Rajakaruna, S., Ma, Z., Gau, V., Anastas, S., Brennan, L.A., Hejtmancik, J.F., Menko, A.S., Kantorow, M., 2014. Differentiation State-specific Mitochondrial Dynamic Regulatory Networks Are Revealed by Global Transcriptional Analysis of the Developing Chicken Lens. G3: Genes|Genomes|Genetics. https://doi.org/10.1534/g3.114.012120.

Chen, J., Ma, Z., Jiao, X., Fariss, R., Kantorow, W.L., Kantorow, M., Pras, E., Frydman, M., Pras, E., Riazuddin, S., Riazuddin, S.A., Hejtmancik, J.F., 2011. Mutations in FYCO1 cause autosomal-recessive congenital cataracts. Am. J. Hum. Genet. 88, 827–838. https://doi.org/10.1016/J.AJHG.2011.05.008.

Chen, Y., Stump, R.J.W., Lovicu, F.J., Shimono, A., McAvoy, J.W., 2008. Wnt signaling is required for organization of the lens fiber cell cytoskeleton and development of lens three-dimensional architecture. Dev. Biol. 324, 161–176. https://doi.org/10.1016/j.ydbio.2008.09.002.

Cheng, C., Nowak, R.B., Fowler, V.M., 2017. The lens actin filament cytoskeleton: Diverse structures for complex functions. Exp. Eye Res. 156, 58–71. https://doi.org/10.1016/j.exer.2016.03.005.

Corces, M.R., Trevino, A.E., Hamilton, E.G., Greenside, P.G., Sinnott-Armstrong, N.A., Vesuna, S., Satpathy, A.T., Rubin, A.J., Montine, K.S., Wu, B., Kathiria, A., Cho, S.W., Mumbach, M.R., Carter, A.C., Kasowski, M., Orloff, L.A., Risca, V.I., Kundaje, A., Khavari, P.A., Montine, T.J., Greenleaf, W.J., Chang, H.Y., 2017. An improved ATAC-seq protocol reduces background and enables interrogation of frozen tissues. Nat. Methods 14, 959–962. https://doi.org/10.1038/nmeth.4396.

Costello, M.J., Brennan, L.A., Basu, S., Chauss, D., Mohamed, A., Gilliland, K.O., Johnsen, S., Menko, A.S., Kantorow, M., 2013. Autophagy and mitophagy participate in ocular lens organelle degradation. Exp. Eye Res. 116, 141–150. https://doi.org/10.1016/j.exer.2013.08.017.

Cvekl, A., Ashery-Padan, R., 2014. The cellular and molecular mechanisms of vertebrate lens development. Development 141, 4432–4447. https://doi.org/10.1242/dev.107953.

Cvekl, A., Zhang, X., 2017. Signaling and gene regulatory networks in mammalian lens development. Trends Genet. 33, 677–702. https://doi.org/10.1016/j.tig.2017.08.001.

FitzGerald, P.G., 2009. Lens intermediate filaments. Exp. Eye Res. 88, 165–172. https://doi.org/10.1016/j.exer.2008.11.007.

Gao, M., Huang, Y., Wang, L., Huang, M., Liu, F., Liao, S., Yu, S., Lu, Z., Han, S., Hu, X., Qu, Z., Liu, X., Assefa Yimer, T., Yang, L., Tang, Z., Li, D.W.-C., Liu, M., 2017. HSF4 regulates lens fiber cell differentiation by activating p53 and its downstream regulators. Cell Death Dis. 8, e3082. https://doi.org/10.1038/cddis.2017.478.

Harrison, P.R., 1990. Molecular mechanisms involved in the regulation of gene expression during cell differentiation and development. Immunol. Ser. 49, 411–464.

He, S., Limi, S., McGreal, R.S., Xie, Q., Brennan, L.A., Kantorow, W.L., Cvekl, A., 2016. Chromatin remodeling enzyme Snf2h regulates embryonic lens differentiation and denucleation. Development (Cambridge, England) 143 (11), 1937–1947. https://doi.org/10.1242/dev.135285.

Horsley, V., Pavlath, G.K., 2002. NFAT: ubiquitous regulator of cell differentiation and adaptation. J. Cell Biol. 156, 771–774. https://doi.org/10.1083/jcb.200111073.

Jia, J., Lin, M., Zhang, L., York, J.P., Zhang, P., 2007. The Notch signaling pathway controls the size of the ocular lens by directly suppressing p57Kip2 expression. Mol. Cell. Biol. 27, 7236–7247. https://doi.org/10.1128/MCB.00780-07.

Jiang, C., Pugh, B.F., 2009. Nucleosome positioning and gene regulation: advances through genomics. Nat. Rev. Genet. 10, 161–172. https://doi.org/10.1038/nrg2522.

Kantorow, M., Cvekl, A., Sax, C.M., Piatigorsky, J., 1993. Protein-DNA interactions of the mouse αA-crystallin control regions: differences between expressing and non-expressing cells. J. Mol. Biol. 230, 425–435. https://doi.org/10.1006/jmbi.1993.1160.

Karolchik, D., Hinrichs, A.S., Furey, T.S., Roskin, K.M., Sugnet, C.W., Haussler, D., Kent, W.J., 2004. The UCSC Table Browser data retrieval tool. Nucleic Acids Res. 32, 493D–496D. https://doi.org/10.1093/nar/gkh103.

Khan, A., Fornes, O., Stigliani, A., Gheorghe, M., Castro-Mondragon, J.A., van der Lee, R., Bessy, A., Chèneby, J., Kulkarni, S.R., Tan, G., Baranasic, D., Arenillas, D.J., Sandelin, A., Vandepoele, K., Lenhard, B., Ballester, B., Wasserman, W.W., Parcy, F., Mathelier, A., 2018. JASPAR 2018: update of the open-access database of

transcription factor binding profiles and its web framework. Nucleic Acids Res. 46, D260–D266. https://doi.org/10.1093/nar/gkx1126.
Lachke, S.A., Alkuraya, F.S., Kneeland, S.C., Ohn, T., Aboukhalil, A., Howell, G.R., Saadi, I., Cavallesco, R., Yue, Y., Tsai, A.C.-H., Nair, K.S., Cosma, M.I., Smith, R.S., Hodges, E., Alfadhli, S.M., Al-Hajeri, A., Shamseldin, H.E., Behbehani, A., Hannon, G.J., Bulyk, M.L., Drack, A.V., Anderson, P.J., John, S.W.M., Maas, R.L., 2011. Mutations in the RNA granule component TDRD7 cause cataract and glaucoma. Science 331, 1571–1576. https://doi.org/10.1126/science.1195970.
Lawrence, M., Daujat, S., Schneider, R., 2016. Lateral thinking: how histone modifications regulate gene expression. Trends Genet. 32, 42–56. https://doi.org/10.1016/j.tig.2015.10.007.
Lovicu, F.J., McAvoy, J.W., 2005. Growth factor regulation of lens development. Dev. Biol. 280, 1–14. https://doi.org/10.1016/j.ydbio.2005.01.020.
Lovicu, F.J., McAvoy, J.W., de Iongh, R.U., 2011. Understanding the role of growth factors in embryonic development: insights from the lens. Philos. Trans. R. Soc. Lond. B Biol. Sci. 366, 1204–1218. https://doi.org/10.1098/rstb.2010.0339.
Martinez, G., Wijesinghe, M., Turner, K., Abud, H.E., Taketo, M.M., Noda, T., Robinson, M.L., de Iongh, R.U., 2009. Conditional mutations of β-catenin and APC reveal roles for canonical Wnt signaling in lens differentiation. Investig. Opthalmol. Vis. Sci. 50, 4794. https://doi.org/10.1167/iovs.09-3567.
Mathias, R.T., White, T.W., Gong, X., 2010. Lens gap junctions in growth, differentiation, and homeostasis. Physiol. Rev. 90, 179–206. https://doi.org/10.1152/physrev.00034.2009.
McAvoy, J.W., Dawes, L.J., Sugiyama, Y., Lovicu, F.J., 2017. Intrinsic and extrinsic regulatory mechanisms are required to form and maintain a lens of the correct size and shape. Exp. Eye Res. 156, 34–40. https://doi.org/10.1016/j.exer.2016.04.009.
McLeay, R.C., Bailey, T.L., 2010. Motif Enrichment Analysis: a unified framework and an evaluation on ChIP data. BMC Bioinf. 11, 165. https://doi.org/10.1186/1471-2105-11-165.
Medina-Martinez, O., Jamrich, M., 2007. Foxe view of lens development and disease. Development 134, 1455–1463. https://doi.org/10.1242/dev.000117.
Meng, F., Li, J., Yang, X., Yuan, X., Tang, X., 2018. Role of Smad3 signaling in the epithelial-mesenchymal transition of the lens epithelium following injury. Int. J. Mol. Med. 42, 851–860. https://doi.org/10.3892/ijmm.2018.3662.
Menko, S.A., 2002. Lens epithelial cell differentiation. Exp. Eye Res. 75, 485–490. https://doi.org/10.1006/exer.2002.2057.
Mi, H., Huang, X., Muruganujan, A., Tang, H., Mills, C., Kang, D., Thomas, P.D., 2017. PANTHER version 11: expanded annotation data from Gene Ontology and Reactome pathways, and data analysis tool enhancements. Nucleic Acids Res. 45, D183–D189. https://doi.org/10.1093/nar/gkw1138.
Moskowitz, D.M., Zhang, D.W., Hu, B., Le Saux, S., Yanes, R.E., Ye, Z., Buenrostro, J.D., Weyand, C.M., Greenleaf, W.J., Goronzy, J.J., 2017. Epigenomics of human CD8 T cell differentiation and aging. Sci. Immunol. 2. https://doi.org/10.1126/sciimmunol.aag0192.
Perng, M.-D., Zhang, Q., Quinlan, R.A., 2007. Insights into the beaded filament of the eye lens. Exp. Cell Res. 313, 2180–2188. https://doi.org/10.1016/j.yexcr.2007.04.005.
Piatigorsky, J., 1981. Lens differentiation in Vertebrates: a review of cellular and molecular features. Differentiation 19, 134–153. https://doi.org/10.1111/J.1432-0436.1981.TB01141.X.
Ramirez, R.N., El-Ali, N.C., Mager, M.A., Wyman, D., Conesa, A., Mortazavi, A., 2017. Dynamic gene regulatory networks of human myeloid differentiation. Cell Sys. 4, 416–429 e3. https://doi.org/10.1016/j.cels.2017.03.005.
Rao, P.V., Maddala, R., 2006. The role of the lens actin cytoskeleton in fiber cell elongation and differentiation. Semin. Cell Dev. Biol. 17, 698–711. https://doi.org/10.1016/j.semcdb.2006.10.011.
Robinson, M.L., 2006. An essential role for FGF receptor signaling in lens development. Semin. Cell Dev. Biol. 17, 726–740. https://doi.org/10.1016/j.semcdb.2006.10.002.
Robinson, M.L., Overbeek, P.A., Verran, D.J., Grizzle, W.E., Stockard, C.R., Friesel, R., Maciag, T., Thompson, J.A., 1995. Extracellular FGF-1 acts as a lens differentiation factor in transgenic mice. Development 121.
Rowan, S., Conley, K.W., Le, T.T., Donner, A.L., Maas, R.L., Brown, N.L., 2008. Notch signaling regulates growth and differentiation in the mammalian lens. Dev. Biol. 321, 111–122. https://doi.org/10.1016/j.ydbio.2008.06.002.
Roy, S., Kundu, T.K., 2014. Gene regulatory networks and epigenetic modifications in cell differentiation. IUBMB Life 66, 100–109. https://doi.org/10.1002/iub.1249.
Rudnizky, S., Malik, O., Bavly, A., Pnueli, L., Melamed, P., Kaplan, A., 2017. Nucleosome mobility and the regulation of gene expression: insights from single-molecule studies. Protein Sci. 26, 1266–1277. https://doi.org/10.1002/pro.3159.
Serrano-Pérez, M.C., Fernández, M., Neria, F., Berjón-Otero, M., Doncel-Pérez, E., Cano, E., Tranque, P., 2015. NFAT transcription factors regulate survival, proliferation, migration, and differentiation of neural precursor cells. Glia 63, 987–1004. https://doi.org/10.1002/glia.22797.
Shi, Y., De Maria, A., Bennett, T., Shiels, A., Bassnett, S., 2012. A role for epha2 in cell migration and refractive organization of the ocular lens. Investig. Ophthalmol. Vis. Sci. 53, 551–559. https://doi.org/10.1167/iovs.11-8568.
Shi, Y., De Maria, A., Lubura, S., iki, H., Bassnett, S., 2015. The penny pusher: a cellular model of lens growth. Investig. Ophthalmol. Vis. Sci. 56, 799–809. https://doi.org/10.1167/iovs.14-16028.
Shui, Y.-B., Arbeit, J.M., Johnson, R.S., Beebe, D.C., 2008a. HIF-1: an age-dependent regulator of lens cell proliferation. Investig. Ophthalmol. Vis. Sci. 49, 4961–4970. https://doi.org/10.1167/iovs.08-2118.
Shui, Y.-B., Arbeit, J.M., Johnson, R.S., Beebe, D.C., 2008b. HIF-1: an age-dependent regulator of lens cell proliferation. Investig. Opthalmol. Vis. Sci. 49, 4961. https://doi.org/10.1167/iovs.08-2118.
Smith, A.N., Miller, L.-A., Radice, G., Ashery-Padan, R., Lang, R.A., 2009. Stage-dependent modes of Pax6-Sox 2 epistasis regulate lens development and eye morphogenesis. Development 136, 3377. https://doi.org/10.1242/dev.043802.
Song, J.Y., Park, R., Kim, J.Y., Hughes, L., Lu, L., Kim, S., Johnson, R.L., Cho, S.-H., 2014. Dual function of Yap in the regulation of lens progenitor cells and cellular polarity. Dev. Biol. 386, 281–290. https://doi.org/10.1016/j.ydbio.2013.12.037.
Stump, R.J., Ang, S., Chen, Y., von Bahr, T., Lovicu, F.J., Pinson, K., de Iongh, R.U., Yamaguchi, T.P., Sassoon, D.A., McAvoy, J.W., 2003. A role for Wnt/β-catenin signaling in lens epithelial differentiation. Dev. Biol. 259, 48–61. https://doi.org/10.1016/S0012-1606(03)00179-9.
Sun, J., Rockowitz, S., Xie, Q., Ashery-Padan, R., Zheng, D., Cvekl, A., 2015. Identification of *in vivo* DNA-binding mechanisms of Pax6 and reconstruction of Pax6-dependent gene regulatory networks during forebrain and lens development. Nucleic Acids Res. 43, 6827–6846. https://doi.org/10.1093/nar/gkv589.
Suzuki-Kerr, H., Baba, Y., Tsuhako, A., Koso, H., Dekker, J.D., Tucker, H.O., Kuribayashi, H., Watanabe, S., 2017. Forkhead box protein P1 is dispensable for retina but essential for lens development. Investig. Opthalmol. Vis. Sci. 58, 1916. https://doi.org/10.1167/iovs.16-20085.
Tuteja, G., Kaestner, K.H., 2007a. SnapShot:Forkhead transcription factors I. Cell 130, 1160.e1-1160.e2. https://doi.org/10.1016/j.cell.2007.09.005.
Tuteja, G., Kaestner, K.H., 2007b. SnapShot: forkhead transcription factors II. Cell 131, 192–192.e1. https://doi.org/10.1016/j.cell.2007.09.016.
Venkatesh, S., Workman, J.L., 2015. Histone exchange, chromatin structure and the regulation of transcription. Nat. Rev. Mol. Cell Biol. 16, 178–189. https://doi.org/10.1038/nrm3941.
Walker, J.L., Menko, A.S., 1999. alpha 6 Integrin is regulated with lens cell differentiation by linkage to the cytoskeleton and isoform switching. Dev. Biol. 210, 497–511. https://doi.org/10.1006/dbio.1999.9277.
Walker, J.L., Zhang, L., Menko, A.S., 2002. A signaling role for the uncleaved form of α6 integrin in differentiating lens fiber cells. Dev. Biol. 251, 195–205. https://doi.org/10.1006/DBIO.2002.0823.
Wang, Q., Zhou, Y., Jackson, L.N., Johnson, S.M., Chow, C.-W., Evers, B.M., 2011. Nuclear factor of activated T cells (NFAT) signaling regulates PTEN expression and intestinal cell differentiation. Mol. Biol. Cell 22, 412–420. https://doi.org/10.1091/mbc.e10-07-0598.
Wistow, G., 2012. The Human Crystallin Gene Families.
Xu, X., Weinstein, M., Li, C., Naski, M., Cohen, R.I., Ornitz, D.M., Leder, P., Deng, C., 1998. Fibroblast growth factor receptor 2 (FGFR2)-mediated reciprocal regulation loop between FGF8 and FGF10 is essential for limb induction. Development 125, 753–765.
Yang, C., Yang, Y., Brennan, L., Bouhassira, E.E., Kantorow, M., Cvekl, A., 2010. Efficient generation of lens progenitor cells and lentoid bodies from human embryonic stem cells in chemically defined conditions. FASEB J. 24, 3274–3283. https://doi.org/10.1096/fj.10-157255.
Zhao, Y., Zheng, D., Cvekl, A., 2018a. A comprehensive spatial-temporal transcriptomic analysis of differentiating nascent mouse lens epithelial and fiber cells. Exp. Eye Res. 175, 56–72. https://doi.org/10.1016/j.exer.2018.06.004.
Zhao, Y., Zheng, D., Cvekl, A., 2018b. A comprehensive spatial-temporal transcriptomic analysis of differentiating nascent mouse lens epithelial and fiber cells. Exp. Eye Res. 175, 56–72. https://doi.org/10.1016/J.EXER.2018.06.004.